VILNIUS UNIVERSITY
FACULTY OF PHYSICS
INSTITUTE OF PHOTONICS AND NANOTECHNOLOGY

Silvija Keraitytė

Optimization of Quantum Structure Technology for Near-Infrared Laser Sources

BACHELOR THESIS

Light Engineering study programme

Student Silvija Keraitytė

Supervisor Assoc. Prof. Dr. Renata Butkutė

Representative of Institute Assoc. Prof. Zigmas Balevičius

Vilnius 2023

Contents

List of Abbreviations 3
Work Contribution 4
Publications of results 4
1. Introduction 6
2. Literature overview 8
  2.1 Quantum Structures 8
  2.2 Vertical-external-cavity surface-emitting laser structure 9
  2.3 Strained Layers 10
  2.4 Molecular Beam Epitaxy 12
  2.5 Principal characterization of Quantum Structures 15
    2.5.1 Photoluminescence 15
    2.5.2 Atomic Force Microscopy 17
    2.5.3 X-Ray Diffraction 18
3. Preparation and growth of the samples 19
4. Experimental results and discussion 22
  4.1 Surface morphology analysis 22
  4.2 X-Ray Diffraction analysis 26
  4.3 Photoluminescence measurements 29
    4.3.1 Room temperature PL 30
    4.3.2 Temperature-dependent PL 37
  4.4 VECSEL structures 39
5. Conclusions 45
Bibliography 48
Summary 51
Santrauka 52

List of Abbreviations

AFM – Atomic force microscopy

BEP – Beam equivalent pressure

DBR – Distributed Bragg reflector

DPSS(L) – Diode-pumped solid-state (laser)

FWHM – Full width at half maximum

HR-XRD – High resolution X-ray diffraction

LiDAR – Laser imaging detection and ranging

MBE – Molecular beam epitaxy

MQW – Multiple quantum wells

NIR – Near-infrared range

OPSL – Optically pumped semiconductor lasers

PBN – Pyrolytic boron nitride

PL – Photoluminescence

QD – Quantum dot

QW – Quantum well

RC – Rocking curve

RHEED – Reflection high-energy electron diffraction

RMS – Root mean square

RPG – Resonant periodic gain

RT – Room temperature

SDL – Semiconductor disk laser

TDPL – Temperature-dependent photoluminescence

UHV – Ultra high vacuum

VCSEL – Vertical-cavity surface-emitting laser

VECSEL – Vertical-external-cavity surface-emitting laser

XRD – X-ray diffraction

Work Contribution

Experimental part of the thesis that consisted of designing, preparing, and growing the samples was performed personally. The characterization of the grown samples, including AFM, PL, XRD measurements, were conducted by other laboratory workers and were personally overseen and assisted during the experiments. The analysis of the aforementioned experiments has been done individually.

The samples and the assessed results of the structures have been published as part of the Student Research Project, funded by the Research Council of Lithuania (LMTLT). Part of the work has also been orally presented during the 18th Apropos conference (2022) and has won the Young Researchers Awards prize. Some of the findings and results are in the process of being published in an article. Deeper knowledge and understanding as well as practical laboratory activities have also been acquired and presented during the studies at Taiwan International Semiconductor Summer School at National Cheng Kung University (NCKU), Tainan (2022 August).

Publications of results

1. **Silvija Keraitytė**, Andrea Zelioli, Evelina Dudutienė, Monika Jokubauskaitė, Bronislavas Čechavičius, Artūras Suchodolskis, Sandra Stanionytė, Virginijus Bukauskas, Vladimir Astachov, Renata Butkutė, **Growth Optimization and Characterization of MQWs based on InGaAs and GaAsBi for NIR sources**, 18th Apropos conference Advanced Properties and Processes in Optoelectronics Materials and Systems, Vilnius, Lithuania, 5-7 October, 2022 (oral presentation). The presentation and the reseearch have won the Young Researcher Award prize administered by Light Conversion.

2. **Silvija Keraitytė**, Andrea Zelioli, Evelina Dudutienė, Monika Jokubauskaitė, Bronislavas Čechavičius, Artūras Suchodolskis, Sandra Stanionytė, Virginijus Bukauskas, Vladimir Astachov, Renata Butkutė **Growth Optimization and Characterization of MQWs based on InGaAs and GaAsBi for VECSELs and NIR sources**, 12th FizTeCh conference for doctorates and young scientists, Vilnius, Lithuania, 19-20 October, 2022 (poster presentation).

3. **Silvija Keraitytė**, Andrea Zelioli, Arnas Pukinskas, Evelina Dudutienė, Bronislavas Čechavičius, Renata Butkutė, **Optimization of Quantum Structures for Applications in Near-Infrared Sources**, 24th International Conference-School Advanced Materials and Technologies, Palanga, Lithuania, 22-26 August, 2022 (poster presentation).

4. Research project No. P-SV-22-221 (***Kvantinių struktūrų, skirtų artimosios infraraudonosios srities lazeriniams šaltiniams, technologijos optimizavimas***) that was conducted during July and August 2022. The project has received funding from the Research Council of Lithuania (LMTLT).

1. Introduction

Vertical-external-cavity surface-emitting lasers (VECSEL) are a novel group of high-power semiconductor lasers that operate in a wide range from UV to IR wavelengths. Its main component - semiconductor chip - consists of a bandgap engineered gain region and a Distributed Bragg Reflector (DBR). Quantum structures are the most favorable way of changing the desired properties of the prospective device. Quantum structure optimization is deemed to be significantly complex, therefore even for mature material growth, problems arise. Most problems that occur are non-radiative recombination processes, including Auger recombination, defect formation, alloy segregation. These difficulties are different for various materials, therefore, for specific desired lasing properties, separate quantum structures with their own growing peculiarities must be taken into account. The NIR range of 760 – 1200 nm is of the utmost importance as it covers laser applications in medicine, LiDAR and fiber communication systems.

While InGaAs is deemed as a mature technology for laser gain media, its growth process still requires precise optimization as even miniscule change in parameters of the quantum wells significantly change the properties of the active media. Meanwhile GaAsBi is a relatively unexplored alloy with favorable features, for example, large bandgap reduction for a given lattice mismatch with GaAs substrates and intense photoluminescence. GaAsBi based structures make an auspicious candidate for long wavelength applications. Specifically for the growth of bismide structures, pressure and growth temperature become extremely important in order to maintain stable Bi/As flux ratio for homogenous growth.

Therefore, the aim of this work is to determine appropriate growth conditions for quantum structures based on InGaAs and GaAsBi materials and optimize their growth procedure that will result in high quality MQW structures for NIR laser devices. The process will lead to a thorough investigation of the effect of growth conditions on GaAsBi and InGaAs optical properties. As such, the obtained results will determine the properties of VECSELs designed for high power operation at 760-1060 nm and 1000-1200 nm wavelength range. Any other findings will base further research and possibly open new possibilities for novel light sources and laser designs.

The main tasks can be described as follows:

1. To optimize the technological parameters for InGaAs MQW structures tailoring the wavelength to 760–1060 nm spectral range.
2. To discover the relationship between technological parameters and optical properties of GaAsBi MQW structures emitting at wavelengths of about 1000-1200 nm.
3. To assess their properties and qualities by analyzing PL, AFM and XRD results.
4. To design and grow full VECSEL structure, and evaluate its optical properties.

2. Literature overview

Once the first laser has been demonstrated back in 1960s [1], numerous types have been developed since, including the most popular and common dye, solid-state and semiconductor lasers. Various configurations have enabled them to be used in a wide range of applications, including medicine, optical fiber communication systems, spectroscopy, materials processing, and many others [2]. Usually, a certain type of laser demonstrates great properties in one way and exhibits limitations in other ways. Yet the most desirable properties of almost any laser are wide wavelength range, good beam quality, i.e., single-transverse mode near-circular beam, high output powers with low threshold. Vertical-external-cavity surface-emitting lasers (VECSEL), also generally referred to as optically pumped semiconductor lasers (OPSL) or semiconductor disk lasers (SDL) are a new group of lasers that offer an elegant alternative to these limitations [1]. They were first developed in the mid-1990s in order to overcome a problem that limits conventional semiconductor lasers namely to expand on the desire to generate high power levels together with perfect transverse mode circular beam quality. These types of lasers also add to the advantage list of generally being compact in size with great efficiency, wide wavelength coverage. Specifically, the external laser cavity enforces output in a low-divergence, circular beam with high quality [1]. In most conventional semiconductor lasers, the gain media comprises of semiconductor material. Most common materials, all exhibiting direct band gap, include GaAs, AlGaAs, GaP, InGaP, InGaAs. As the photon energy is close to the bandgap energy, compositions with different bandgap energies can allow different emission wavelengths. Especially promising gain materials include ternary and quaternary compounds where the increase or the decrease of substance content can change the bandgap energy in certain range [1], [3], [4].

2.1 Quantum Structures

Semiconductor structures in lasers are based on the concept of an active material (e.g., InGaAs or GaAsBi) embedded into another semiconductor with a slightly larger bandgap (e.g., GaAs). The result is a potential well where electrons and holes confine themselves and create higher carrier densities in the active region [5]. Grown microstructures possess different electronic and optical properties from their corresponding bulk materials and in turn promise better performance devices. Therefore, quantum well structures have proven to be superior to bulk materials and are generally used in most semiconductor lasers with layers of 5-10 nm thickness. These structures exhibit quantum confinement that restricts the free carries

movement to two dimensions with the plane of the films that generally have a thickness of several atomic monolayers, i.e., it is comparable or less to the thermal wavelength of the carriers. The result is elimination of any movement perpendicular to the films and the corresponding energy states of the carriers become quantized [6]. Due to the quantum effect, the laser gain bandwidth is reduced. As the energy deposition is also confined to a smaller region over overall smaller volume, the threshold current is significantly reduced yet the laser output power remains unbiased. Quantum confinement effects can also be realized in quantum dots. Even though the growth of QDs is possible with the precision of few degrees, they are still not widely used in semiconductor material, including VECSELs, due to their complexity in nature and lack of research. However, they hold a lot of promise for the future as they can be grown in larger numbers compared to quantum wells and under strained conditions, showing the flexibility of designing the gain medium with more precise emission wavelength [7].

2.2 Vertical-external-cavity surface-emitting laser structure

Namely the most important part of the VECSEL is, just like in any laser, the active region. Structurally it is composed of a highly reflective mirror, a DBR most commonly implemented, and a region with multiple quantum wells, all of which are usually fabricated with an epitaxial process on a semiconductor wafer. A simplified schematic structure of a typical VECSEL gain mirror can be seen in Figure 1.

In general, the single-pass of a vertical cavity quantum well is small due to the short interaction length between the laser mode and the gain material. This however can be compensated by using a larger number of quantum wells. Generally, in semiconductor lasers (including vertical-cavity surface-emitting laser - VCSEL) the threshold current density increases with higher number of quantum wells in the gain medium [5]. The most optimal number of quantum well is generally defined to be 3, exhibiting lowest threshold, whereas the increase of quantum wells above 5 shows higher undesirable threshold current densities [8]. This, however, is different for VECSEL structures, because the optimization can be achieved by placing the QWs periodically at the antinodes of the optical standing wave that is formed in the semiconductor cavity together confined by the DBR and the top surface. Such composition is called a resonant periodic gain (RPG) architecture but other alternatives are possible and can include various designs of QWs or inhomogeneous broadened QD-based gain regions, which also enhance the wavelength tunability [3]. As a result, the design and structure of the active

region enables the use of various materials and their alloys and compounds to tailor the fundamental properties of the VECSEL or other NIR sources.

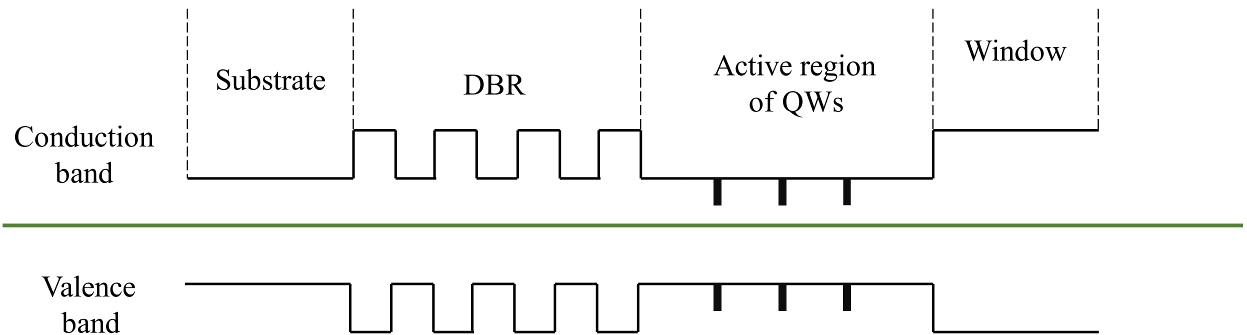

Figure 1. Schematic depiction of a VECSEL structure. The VECSEL structure consists of the highly reflecting semiconductor Bragg mirror, the active region containing several quantum wells separated by barriers (which absorb the pump radiation) and on top a window layer is grown, which prevents the photogenerated carriers from nonradiative recombination on the surface.

2.3 Strained Layers

As the active region and DBR mirror are grown one after another, lattice constants of all semiconductor materials should be matched to each other, although some lattice mismatch – strain – is allowed and may have benefits in certain condition [4]. Even though some lattice strain per QW can be favourable in terms of increasing the differential gain as it lifts the heavy and light hole degeneracy in the valence band reducing the density of states, VECSELs generally require more than 10 QWs [3]. This strain that results in using multiple QW structures can be compensated by growing layers that have opposite strain compared to the desired structure. The strain compensation technique results in decreased lasing threshold. For example, in the case of InGaAs QWs the compressive strain can be compensated by placing GaAsP layers at the nodes of the optical field in the RPG mirror [3]. Another approach could be to alloy small content of nitrogen into the QWs as it would lengthen the emission wavelength without additional strain [9]. However, GaAsBi are an unexplored field of alloys, especially regarding their use as active gain media for semiconductor lasers and NIR sources. One of the more early investigations of GaAsBi have already contended important characteristics and a new concept of having a GaAsBi alloy to create a laser with a temperature insensitive bandgap has emerged [10]. This greatly motivated the field ever since, as a laser with a temperature insensitive emission wavelength would have profound implications in the telecommunications

industry. This becomes a complex technological obstacle as Bi tends to segregate easily and low substrate temperatures are needed for proper Bi atom incorporation into the structures [11]. And while there are not many attempts at implementing this material into VECSEL technologies, they do, however, possess favourable properties regarding applications of light sources at longer wavelengths [12].

It is important for the grown media used in semiconductor lasers to be as perfect as possible and to avoid any possible defects and dislocations. If any defects appear in the crystal, they can function as nonradiative recombination centers, including the process of Auger recombination. Since the layers are grown epitaxially on the substrate it is important to know that the substrate and the lattice constant of the layer material need to be as similar as possible. If these constants do not meet, a lattice mismatch occurs, and the certain amount of strain develops between the layers. The strain becomes more defined with the increase of the lattice mismatch. If there is too much strain present, the probability for dislocation defects to appear rises [2]. These dislocations are especially essential for applications including lasers and wide-gap AIII-BV group materials in general.

However, it has been demonstrated that it is possible to deliberately introduce a certain amount of strain into the quantum wells without causing an influx of dislocations [13]. This induced strain created benefits such as a significant reduction in threshold current, increased output powers and operating bandwidth, decreased chirp, linewidth [14]. In addition to these merits, this ability to grow layers that do not inherently need to match the lattice constant to the substrate, allow the freedom of many new material compositions and alloys. Therefore, the possibility to grow layers under strained conditions, such as quantum wells, can make the laser gain medium design more flexible regarding the emission wavelength [15]. InGaAs as a material is well-developed field and has been deemed as a suitable candidate for high-performance VECSELs operating up to 1 μm. Most widely used material with specifically strained InGaAs quantum wells is GaAs barrier, while AlGaAs can be used to formed deeper wells [1], [16]. In a similar sense, GaAsBi, a relatively recent material system, may be seen as an alternative to InGaAs. Alloying GaAs with Bi results in a large band gap reduction for only a small concentration of Bi, ~ 75 meV/% Bi [17] (~ 620 meV/% strain on GaAs). This is significantly larger than the ~ 15 meV/% In [18] (240 meV/% strain on GaAs) reduction with the incorporation of In. The required low growth temperature of less than 400°C also means that excess Bi will form Bi droplets rather than evaporate, requiring a controlled Bi flux. However even given these difficulties it still makes GaAsBi a very appealing material in terms

of wavelength extension regarding longer than 1 μm wavelength applications in NIR sensors, transistors, THz emitters and detectors.

2.4 Molecular Beam Epitaxy

Molecular beam epitaxy (MBE) is an elegant material growth technique, often described as a physical thin film deposition technique, that offers crystalline high quality films grown in ultra-high vacuum (UHV) (typically higher than 10^{-10} torr) with precise control of thickness, composition, purity, and interface formation [7]. Epitaxy is the arrangement of one or more thermal particles on top of a heated substrate to form a thin layer of a material that could be different from the substrate but with a matched crystallinity of the layers. The key features that distinguish the MBE from other growth techniques is the high degree of control and reproducibility of various complex crystals as well as the possibility to study crystal growth in an in-situ fashion and on a subnanometer scale. Main growth characteristics include low growth rate of around 1 monolayer per second and low growth temperatures [19].

a)

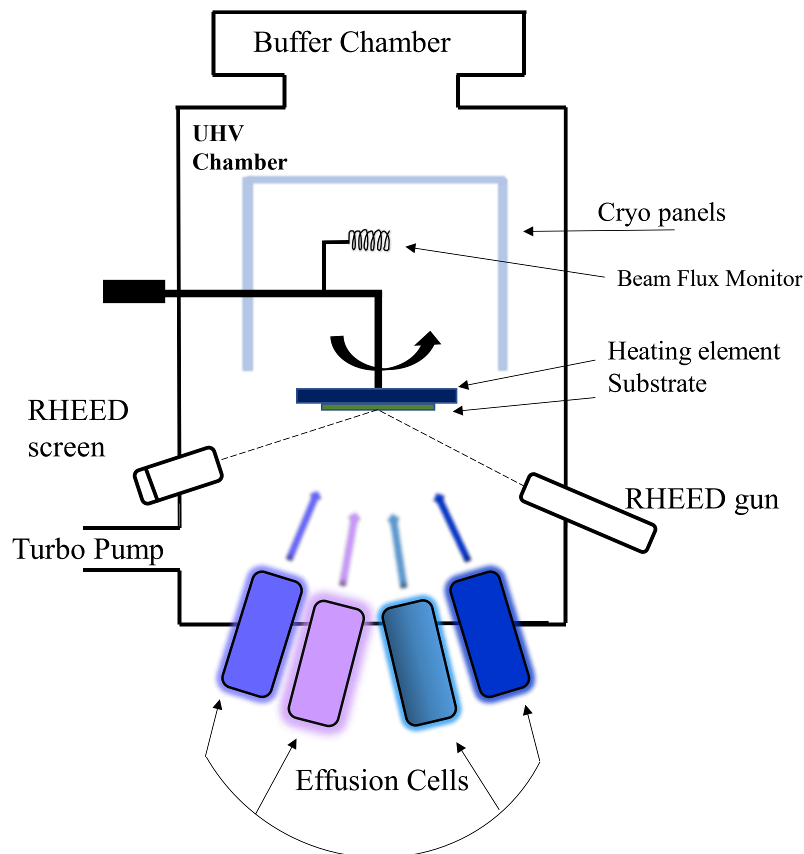

b)

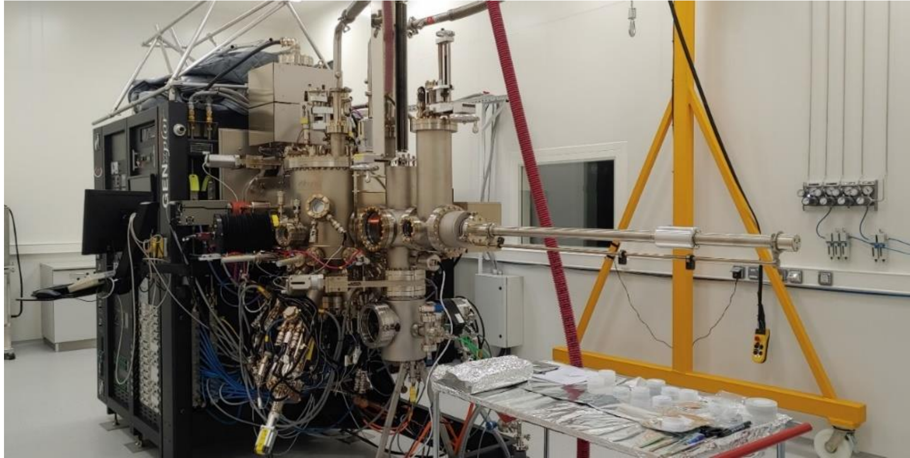

Figure 2. a) Schematic representation of the MBE system. b) MBE Veeco GENxplor system. Main Ultra-High-Vacuum chamber consists of turbo pump and cryo panels for cooling, effusion cells with deposition materials, rotating substrate holder with beam flux monitor and RHEED gun with phosphorescent screen.

The growth chamber consists of effusion (or Knudsen) cells that hold material compounds or components. The crucibles are usually made from pyrolytic boron nitride (PBN) that can withstand up to 1400 ℃ without affecting the material dissociation on the grown layers and supplying beams that generally have thermal energy. The standard effusion cells are limited to be operated under 1200 ℃ which is just enough for Si, Al, Ga evaporation. An overall simplified scheme is shown in Fig. 2 a.

Main deposition process of the epitaxial growth begins with the adsorption of the atoms that impinge on the surface and their dissociation with surface diffusion. The atoms eventually arrange themselves onto the crystal lattice meanwhile the atoms that do not structuralize desorb thermally [15]. In general, the grown layers have the same crystalline structure of the substrate or a structure with a similar symmetry and a lattice parameter that differs from that of the substrate only by a non-substantial amount (around 10%).

For an *in-situ* monitoring of the thin films epitaxial growth, the system uses high-energy electron diffraction (RHEED) that uses a small glancing angle reflection mode of the operation. The main feature of RHEED is that the angle is extremely sensitive to the uppermost layers rather than the bulk structure. This enables a way to monitor the growth structure and the morphology of the layer without interfering and disrupting the growth process [15]. It is based on an incident electron beam that strikes the layer of the sample with an exceedingly small, grazing angle (~3°) that then reflects onto the phosphorescent screen which then can be analysed (Fig. 3).

If the surface of the layer is not smooth and flat, electrons transmit through the surface and scatter in different directions resulting in a RHEED pattern that is characterized by uneven spots. This is especially important at the beginning of the growth where the substrate or the base layer has oxides on the surface. Meanwhile the diffraction that originates from a perfectly flat surface will result in a pattern consisting of elongated streaks with modulated intensity due to inelastically scattered electrons. RHEED analysis also provides information regarding the diffraction from an amorphous surface (oxides formed on the substrate), in which case no diffraction pattern could be observed at all. RHEED pattern formed on the epi-ready substrate during the beginning of the growth procedure and after oxide desorption is depicted in Figure 4. The visible 2x4 patterns in Fig. 4 (c) and (d) confirm successful oxide desorption from the surface. This means that further growth of the buffer layer can be realised. Kikuchi lines, which form due to electron scattering, are also present in Fig. 4 (c) and (d) and can be used to determine the crystal orientation. Kikuchi lines also originate from high crystalline surfaces, with little dislocations. The distance between the streaks of RHEED pattern is also an indication of the reciprocal surface lattice unit cell size [20]. Therefore, a clean substrate is a vital prerequisite for epitaxial growth, since its oxidation due to atmospheric exposure will cause crystal defects and degrade both optical and electrical properties of the layers.

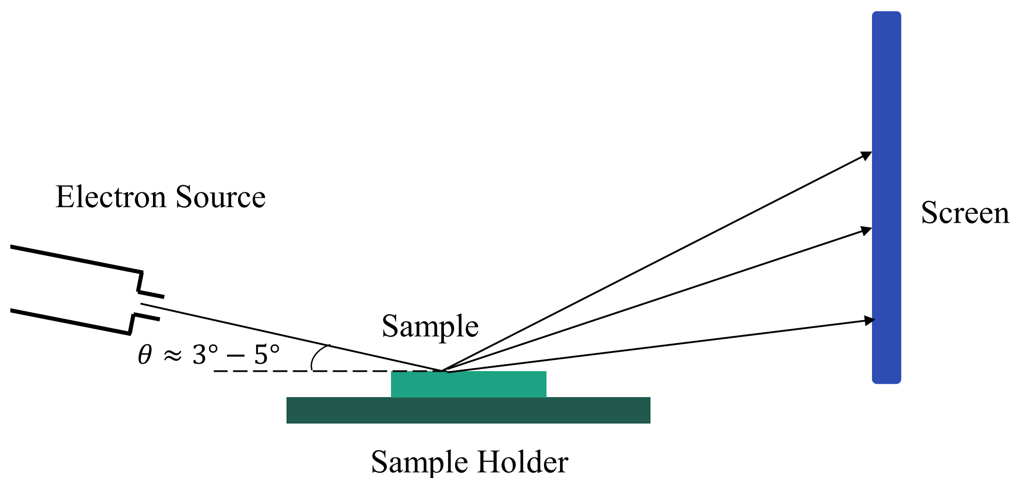

Figure 3. Schematic of a RHEED setup. High energy photons are emitted at a small grazing angle towards the sample surface, from which the scattering can be observed on a fluorescent screen.

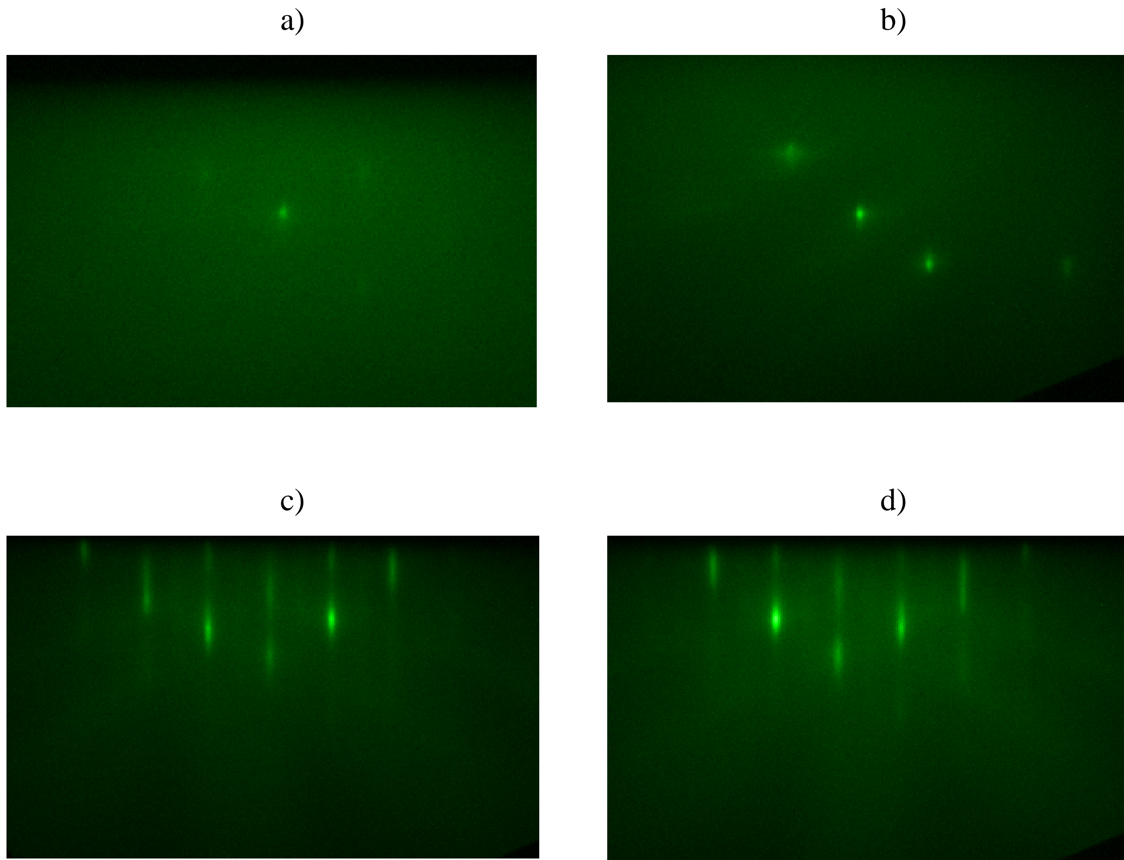

Figure 4. RHEED pattern of epilayer GaAs substrate before (a, b) oxide desorption and after (c, d) indicating a 2x4 pattern and a clean surface ready for the growth of buffer layer. Visible faint Kikuchi lines in (c, d) also depict high crystalline quality surface.

2.5 Principal characterization of Quantum Structures

2.5.1 Photoluminescence

Photoluminescence (PL) is deemed as powerhouse optical characterization techniques due to its ability to yield valuable information regarding intrinsic and extrinsic transitions. It is extremely sensitive to subband electron transitions and transitions to defect-related bands and in addition method itself is simple, non-destructive and does not require any special preparation of the sample. The excitation of the sample with a focused or non-focused laser beam that specifically has higher photon energies than the bandgap energy, generate electrons and holes. As they relax and transition to lower energy states they can recombine and emit photons. Photoluminescence spectra enable the determination of the nature of electronic transitions and the electronic structure as well as various processes of the material under study. Band-to-band transitions yield information about the bandgap as well.

A quite simple schematic of the setup is shown in Fig. 5 below.

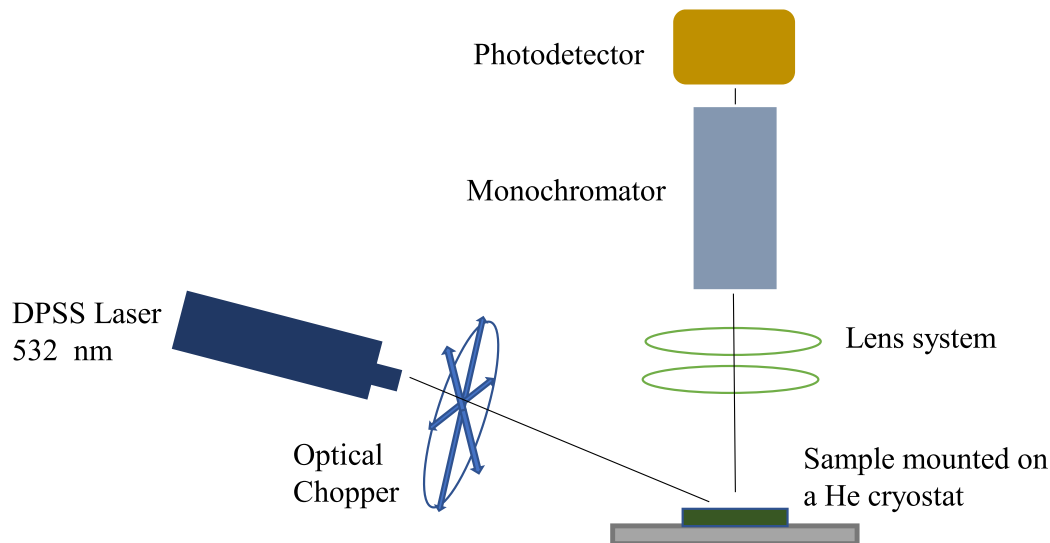

Figure 5. A simplified schematic of a photoluminescence measurement setup. The setup contains a sample, which is placed in a closed-cycle He cryostat with a temperature controller for TDPL measurements. The samples are excited by a DPSS laser of 532 nm with an output power of 190 mW and with an optical chopper wheel, whereas the signal is detected through a thermoelectrically cooled InGaAs photodetector. All measurements were taken in the low photon energy range of 0.9-1.4 eV.

Most samples were characterized in room temperature. For this, a diode-pumped solid-state laser emitting at a wavelength of 532 nm at 190 mW was used as an excitation source at different excitation powers. PL signal was detected with a thermoelectrically cooled InGaAs photodetector using a conventional lock-in system. For specific samples of both, GaAsBi and InGaAs, structures measurements were taken from 3K to 300K to specify the temperature-dependent PL behavior. Similarly, the signal was analyzed in the low photon energy range of 0.9-1.4 eV. For low temperature measurements an open-cycle cryostat, cooled by liquid nitrogen has been used. This characterization determined the dominating recombination mechanism of the structure. Usually in quantum structures the most probable recombination is Auger recombination process, which transposes radiative recombination losses and in turn deteriorate the luminescence of the quantum structures and restrict their applications in lasers, diodes, and such.

2.5.2 Atomic Force Microscopy

Atomic Force Microscopy (AFM) is based on using a tip that interacts with the sample's surface via contact forces. The deflection of the cantilever that the tip is attached to will yield information regarding the interaction force between the tip and the sample thus revealing the morphology of the surface. The deflection is measured using a laser and a photodetector. Meaning that the position of the laser reflection on the detector yield information on the deflection of the cantilever. The tip is moved across the system using a scanner made of a piezoelectric material, which allows for precise movement of the tip. This allows the scanning system of the AFM measurement to reach a resolution of nanometers in the xy plane and sub nanometer sensibility in the z direction. A simplified scheme is shown in Fig. 6.

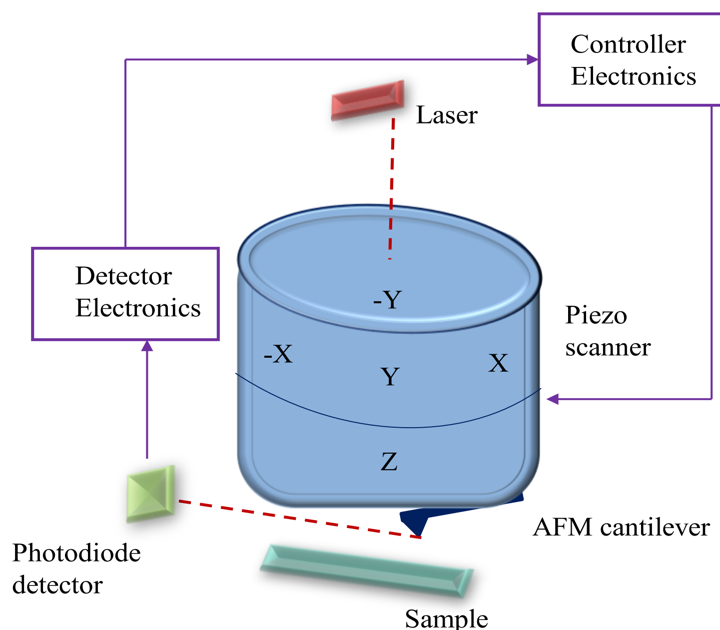

Figure 6. A simplified schematic of an atomic force microscopy setup. The AFM cantilever is placed onto the cylindrical piezo scanner mounted near the top of the microscope. Constant deflection of the AFM cantilever can be maintained by the feedback loop of the system. The information about the sample is directed towards the detector.

AFM measurements can be done in three modes: contact, non-contact and tapping. For the analyzed samples, the tapping was done in air, revealing a topographic map of the surface without damaging it as the cantilever with the tip quivers along the resonant frequency. In addition, with this AFM method, it is possible to separate a well from a formed droplet, as the cantilever tip registers every position of the surface. The results also let the program determine the RMS value, which evaluated the quality of the sample surface even further. In this work, all the samples were characterized by scanning probe AFM Veeco Dimension 3100.

2.5.3 X-Ray Diffraction

The modelling of the quantum well gain media can also be done using X-ray Diffraction (XRD). The samples were characterized using HR-XRD diffractometer, using Bruker D8 Advance system, which according to the rocking curves, the content of the structure has been determined. All samples are characterized using the ω-2θ coupled scans in order to reveal their parameters and lattice crystallographic structure.

A simplified scheme of a XRD RC setup is depicted in Fig. 7.

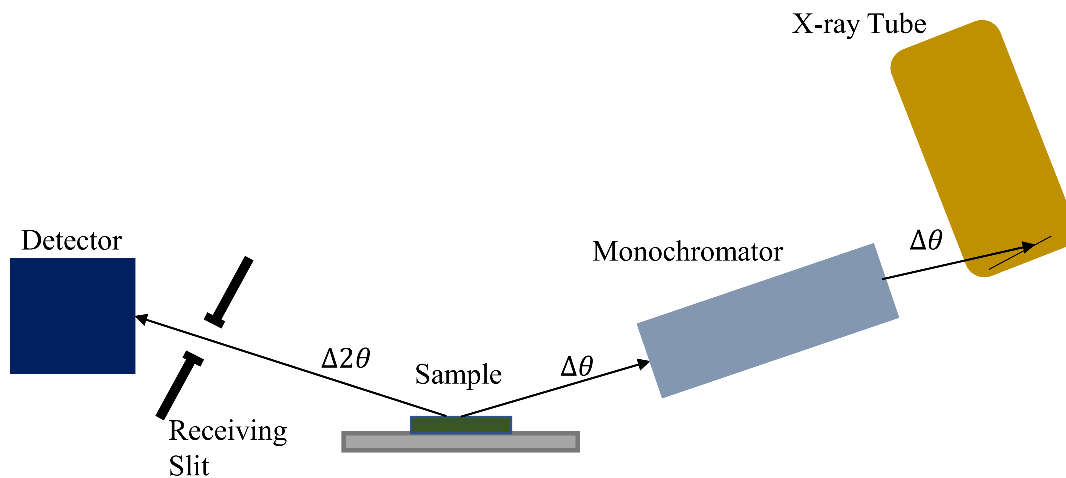

Figure 7. Scheme of a XRD Rocking Curve analysis setup. An X-ray source is used to generate a high intensity X-ray beam, a monochromator is used for selecting specific emission line (e.g., $Cu_{K\alpha 1}$). The intensity of the diffracted beam that characterizes the lattice is measured by a CCD detector. A slit defines the size of incident X-ray beam.

Rocking curves itself are primarily used to study defects such as dislocation density, mosaic spread, curvature, misorientation, and inhomogeneity. Whereas in lattice matched thin films, rocking curves can also be used to study layer thickness, superlattice period, strain and composition profile, lattice mismatch, ternary composition, and relaxation. It is also a critical method for the growth of layers if the relaxation is yet not present. Therefore, to get rocking curves, the detector was set at a specific Bragg angle and the sample was tilted at a small angle. If the sample contains a perfect crystal, the results will show a very sharp peak, but only observed if the sample is tilted enough so that the crystallographic direction becomes parallel to the diffraction vector. Meanwhile the broadenings of the rocking curve will indicate defects and curvatures.

The method proves to yield accurate structural characterization the system with active-layer thicknesses down to 0.1 nm. It is also possible to determine other layer thicknesses and interfaces, as well as the structural quality of the media and the interface roughness, helps determine the strain of the layers. To further evaluate the surface quality, the samples were also characterized by reciprocal space mapping (RSM).

3. Preparation and growth of the samples

The samples were grown using Molecular Beam Epitaxy (MBE) systems (Veeco GENxplor R&D, 2015 and SVT "III-V MBE System Model C-V-2") and using the software program that controls the growth procedure. The MBE system is equipped with several standard cells of which metallic indium, aluminium, gallium, bismuth and unique arsenic design source generating pure arsenic dimers flux has been used. Samples were grown on epi-ready semi-insulating GaAs wafers oriented in the (001) crystallographic plane. For optimisation of growth conditions, the samples ¼ 2" of SI - GaAs wafers were used. The number of MQWs for all samples was set at 12 as it was considered to be the most optimal number from earlier growth experience, taking output power as a criterion, and literature [3]. The substrate temperature was measured at all times by a thermocouple with an accuracy of 1ºC. Beam equivalent pressures (BEP), which are essential especially for growth of bismides, were measured by a retractable ion gauge. Prior to the growth of the quantum structures, the substrates' native oxides were outgassed in three chambers under maximum arsenic flux to ensure homogenous layering. The procedure was monitored *in situ* by RHEED, where the reflected patterns of the substrate surface and the buffer layer have been observed on the screen. Revealing a 2x4 striped RHEED pattern similar to shown previously (Fig. 4, c and d) meant that the oxides have been desorbed and the growth procedure can begin. Once the effusion cells are heated enough, the solid material inside starts to sublimate. Then the shutters of the cells are opened, and the atoms diffuse in the chamber and start to condense on to the sample. On the surface, atoms are able to bond with others, meaning deposited gallium and arsenic atoms will form a gallium arsenide layer with the structure that of a single crystal. To obtain highest output power the VECSEL must contain correct design of MQW. The goal of the parameter optimization was to obtain a lattice matched strain-balanced high quality crystalline multiple quantum well structures with sharp interfaces on GaAs substrate.

It is important to note that specifically for the growth of GaAsBi MQWs, it is technologically important to maintain low substrate temperatures, in order to increase Bi incorporation but avoid any Bi segregation as well. Therefore, the as the barriers of the quantum wells were grown at around 425ºC, the substrate temperatures had to be decreased down to around 300ºC, at the same time exposed under Bi flux for short intervals, maintaining the BEP at 1.065-1.085, while the growth rate of GaAsBi for all samples was around 0.2 nm/s. The summary of GaAsBi quantum well technological growth conditions, parameters and full structure design are presented in Fig. 8. b) and Table 2.

The optimization of InGaAs quantum well structures remained as follows. The indium content in the quantum wells was varied between 15 % and 26 % and the thickness was changed from 3.5 nm to 5.5 nm, as the goal was to target the 976-1060 nm emission wavelengths. The substrate temperature during the growth of all samples was kept at 580ºC. The fluxes of different atoms were also measured, that in turn yielded an estimate of In and Ga ratio which were later assumed for the indium content in the InGaAs layer. The growth rate of InGaAs was calibrated to be between 0.8-0.9 monolayers per second for all samples. The summary of grown samples technological and PL parameters as well as the scheme of the structure are presented in Tables 1 and Fig. 8 a, respectively.

The software was used to define each step of the growth process and adjust the needed thickness of the layers by changing the time duration of each step. For that it was obligatory to measure the growth rate. The growth rates are calculated using RHEED system. Obtained intensity oscillations of the diffraction spots allows to estimate growth rate as a number of monolayers grown per second which will later also be used in determining of growth time needed to deposit different thicknesses of QW or barrier layers. RHEED has also been employed to investigate structural variations over surface stoichiometry for epitaxial growth on GaAs surfaces.

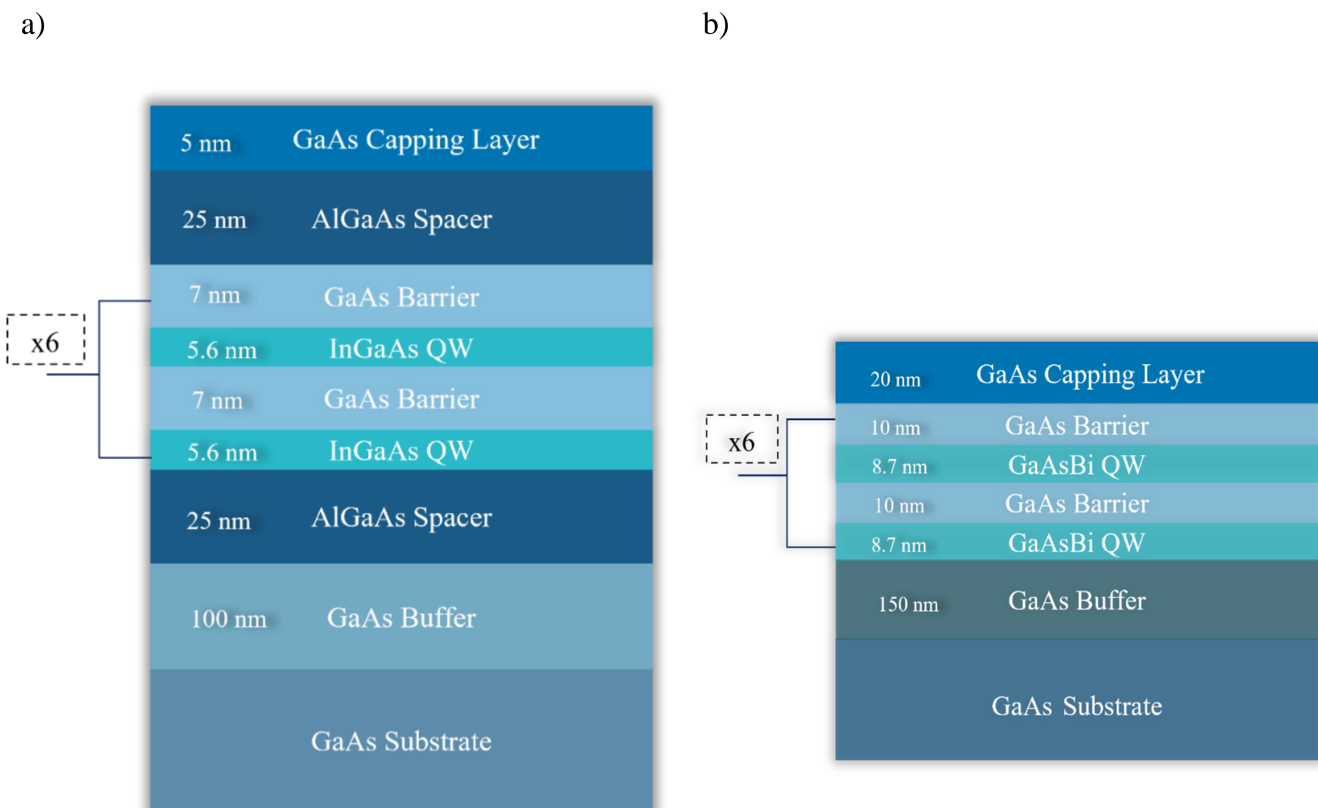

Figure 8. Schematic of structures containing a) InGaAs MQW and b) GaAsBi MQW grown on GaAs substrates using MBE. Both structures contained 12 quantum wells in total and varied in QW parameters.

Table 1. Quantum structures based on InGaAs material: samples and their parameters. The accurate indium content and the quantum well width has been acquired from XRD analysis.

Sample	In/Ga beam flux ratio	In % in QW	Quantum well thickness, nm	Emission wavelength, nm	PL maximum intensity, a.u.
VGA0495	0.739	20.5	5.6	978.9	35140
VGA0918	0.887	23.5	5.1	999.8	150.3
VGA0521	0.912	23.2	5	982	22995
VGA0546	0.997	26	4.95	1002	37405
VGA0919	0.887	22	4.5	998.2	0.3
VGA0920	0.887	25	4.1	985.5	12.4
VGA0512	0.87	22.5	4.1	965	57314
VGA0503	0.993	24	3.6	962	73400
VGA0921	0.887	25	2.85	957.4	5.3

Table 1. Quantum structures based on GaAsBi material: samples and their technological parameters.

Sample	QW Thickness, nm	Energy, eV	Wavelength, nm	Intensity, a.u.	As/Ga	Substrate T, °C
VGA1137	8.7	1.1732	1082.50938	405	1.001884	425
VGA1138	8.7	1.0444	1216.00919	18.04	1.001884	425
VGA1140	8.7	1.0528	1206.30699	23.98	0.9857	425
VGA1141	8.7	1.1486	1105.69389	161.48	0.9857	425
VGA1142	8.7	1.1299	1123.99327	169.03	0.98879	425
VGA1143	7.9	1.097	1157.70283	49.86	0.899173	425
VGA1144	7.9	1.1391	1114.91528	297.2	0.921431	425
VGA1149	7.9	0.967	1313.34023	1.19	0.921431	425
VGA1150	8.6	1.0631	1194.61951	10.52	0.980255	425
VGA1151	7.9	1.105	1149.32127	52.31	0.980255	425
VGA1153	7.9	1.1464	1107.81577	275.83	0.860348	425
VGA1154	7.9	1.1659	1089.28725	188.64	0.846132	445

4. Experimental results and discussion

This section of the thesis will further expand on the characterization of the grown samples and the results' analysis, followed by a discussion.

The grown samples were first characterized by photoluminescence measurements to assess their most important optical properties and surface morphology for overall sample quality. These main results will portray the samples' capabilities and are critical for VECSEL integration. Further studies of XRD have outlined exact structures' parameters. As such this has based the comparison of the samples and their properties. The analysis can be organized in two groups: QW structures based on (1) InGaAs/GaAs and (2) GaAsBi/GaAs, which were grown in their according growth conditions, varying their main QW parameters to achieve high emissions at desired wavelengths and exhibit overall high quality morphology results.

The last part of the section is the investigation of fully designed and grown VECSEL structures. The structures were based on the researched active materials, InGaAs and GaAsBi based MQWs. The section is concluded by their analysis and further assessment.

4.1 Surface morphology analysis

Surface morphology analysis is the basis of all epitaxially grown structures. It enables to qualitatively inspect each and every sample and deduce any surface ministrations, leading to

thorough material behaviour studies. As such, these results are vital for quantum structures that are to be implemented into laser gain media as the surface roughness can influence the intensity of the possible lasing.

The growth mechanism and overall surface roughness of the samples have been characterized *ex situ* by AFM measurements. The microscope was capable of imaging the surface of the samples with a horizontal and vertical resolution down to a fraction of a nanometer. The AFM setup consisted of a cantilever with a sharp tip used to scan the surface of the samples. For all the experiments, the tapping was done in air as it is a convenient mode for multicomponent sample surface imaging. This is due to the fact that the cantilever is vibrated near its resonance frequency causing the tip to oscillate so the probe only comes into close contact with the surface intermittently.

The results carried out on several samples are shown in Figure 9 and 10. The color scale that is presented on all figures on the right various resolutions demonstrates the surface roughness of the samples measured from peak (min) to peak (max). Such results are important for quantum structures. If the sample's surface is evidently rough and many defects cover the surface, further VECSEL implementation is not possible as lasing would not occur from such surface.

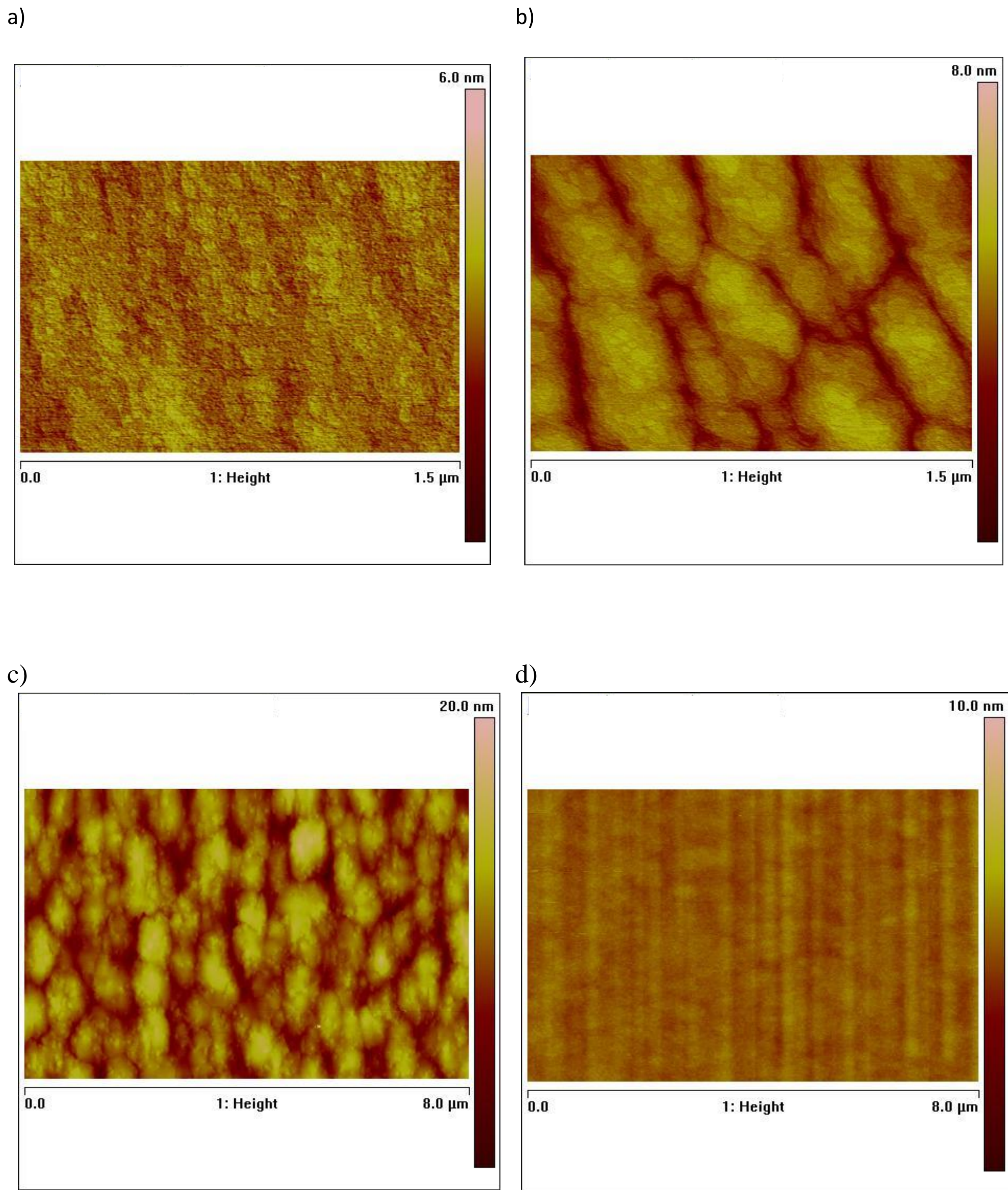

Figure 9. Samples' with active material InGaAs surface investigation using atomic force microscopy: a) VGA1129; b) VGA1130; c) VGA0919; d) VGA0918. The samples were grown in the same ambient conditions, the structures varied only in the In content and QW width. The colour scale on the right shows a scale bar for the height in the images.

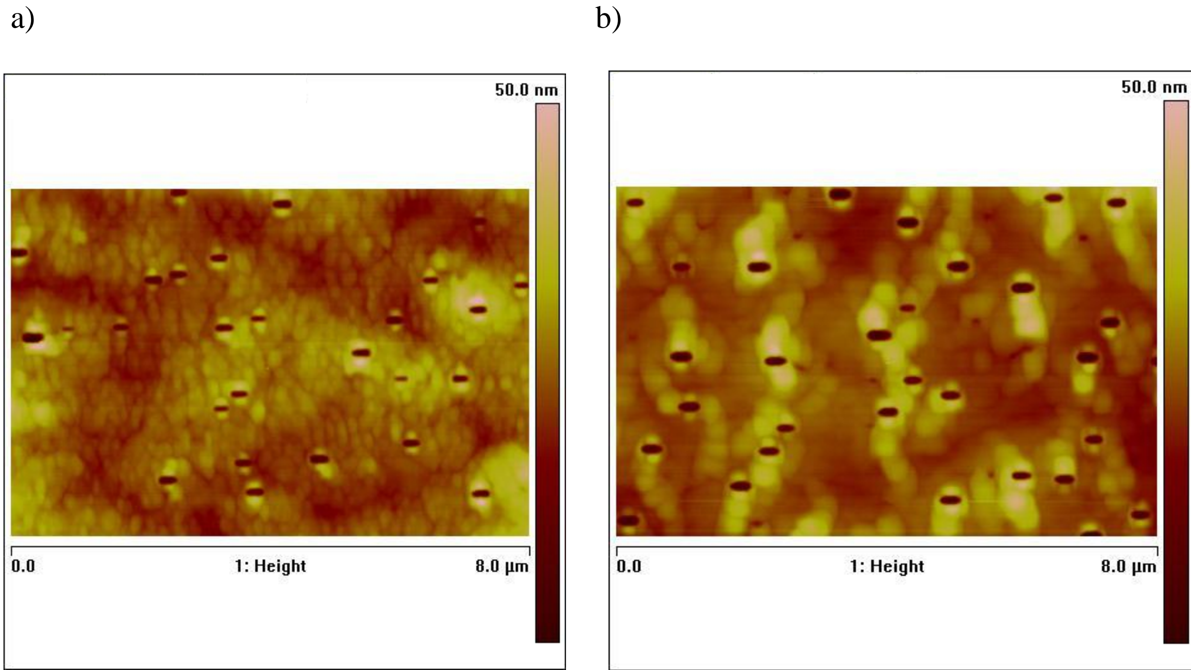

Figure 10. Samples' with active material GaAsBi surface investigation using atomic force microscopy: a) VGA1136; b) VGA1137. The samples were grown under the same conditions (i.e., growth temperature and BEP ratio) with only Bi content and QW width as the varied parameters. Bi concentration of the samples, 7.8% and 4.8% for VGA1136 and VGA1137, respectively, were acquired from XRD scans. The colour scale on the right shows a scale bar for the height in the images.

Figure 9 depicts AFM characterization of samples containing InGaAs MQW structures. All structures had a total of 12 QWs and their parameters varied between 20-23.5% of In content and 4-5 nm of QW width. Layers grown at optimal conditions have shown smooth surface results: most samples' layers have not exceeded 1 nm RMS value (such roughness that does not exceed two crystal lattice width). This is as expected for InGaAs based quantum structures. For specific samples, VGA1130 and VGA0919, surface roughness was higher as well as formed pits have been observed. This might be evidenced by thin buffer layer or not optimized sample surface preparation.

It is also important to note that due to a very narrow window of optimal growth conditions for Bi alloys and its inclination to segregate and form Bi droplets on the surface, even after repeated growth procedures, due to MBE source pressure measuring inaccuracies, it is difficult to obtain superior quality layers without any formations on the surface. Figure 10 depicts AFM characterization of structures containing GaAsBi/GaAs MQWs. Both samples were grown

under the same conditions, where the pressure and substrate temperature has not been changed, and only the Bi incorporation has varied at 7.8% and 4.8%.

AFM results can yield evidence of pits and droplets on the surface. Therefore, visible pits across the surface of both analyzed samples evidence the complexity of the Bi growth optimization. Bismuth excess on the surface is usually defined by pits, characterized by a V shape, which form due to crystallographic structure. This is also due to technological condition inaccuracies, non-optimized Bi/As flow ratio, As deficiency in the layer. Therefore, it has been observed that droplets and formations have segregated on Bi containing sample surfaces, that arguably do influence photoluminescence results.

The roughness of the sample surface varies around 4 - 5 nm. This is even more evident if the Bi/As Beam Equivalent Pressure (BEP) ratio is not fully optimized. Usually as the Bi content in the layers and structures increases and if the parameters are constant, surface roughness still increases. This is especially not desired for structures that are to be implemented into VECSELs. In addition to that, with increasing BEP ratio, as the Bi content increases, the emission wavelength shifts towards longer wavelengths, i.e. the bandgap decreases, enabling the growth of high quality structures beyond 1-1.2 μm [21], [22]. Even though the growth process is complex, and it is difficult to maintain correct parameters, especially during the growth of series of samples. Still, the observed tendencies are in favor with documented literature [23], [24].

4.2 X-Ray Diffraction analysis

XRD scans are important for successful epitaxial growth. They enable the possibility to inspect the strain of the layers that base correct growth of any quantum structures. Furthermore, RC scans analyse the exact parameters of the quantum wells, including layer thicknesses and the amount of components in the structure, that lead to a thorough overview of the structures.

X-ray diffraction (XRD) was also performed on some of the samples in order to determine the thickness and strain of the layers, from which precise indium and bismuth content can be deduced. The epitaxial multilayer structures of the following samples have been studied using the extended rocking curve analysis method. Rocking curves are primarily used to evaluate layer thickness, superlattice period, lattice constant in growth direction.

For these samples, a coupled ω-2θ scan was conducted, in which the direction being measured (scattering vector) does not change. In general, the obtained peaks define the structure of the lattice, i.e., sharper peaks inform about the clean epitaxial ordering of the lattice. The Bragg's peaks and the fringe thicknesses can also be used to quantify the structure's overall thickness. The XRD spectra results are shown in Figure 11.

a)

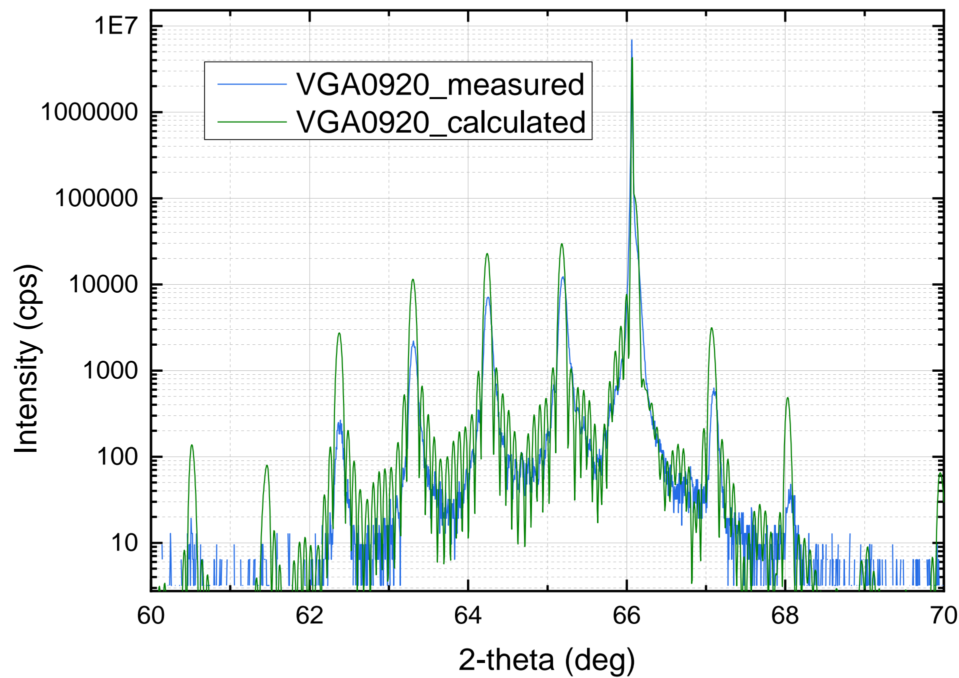

b)

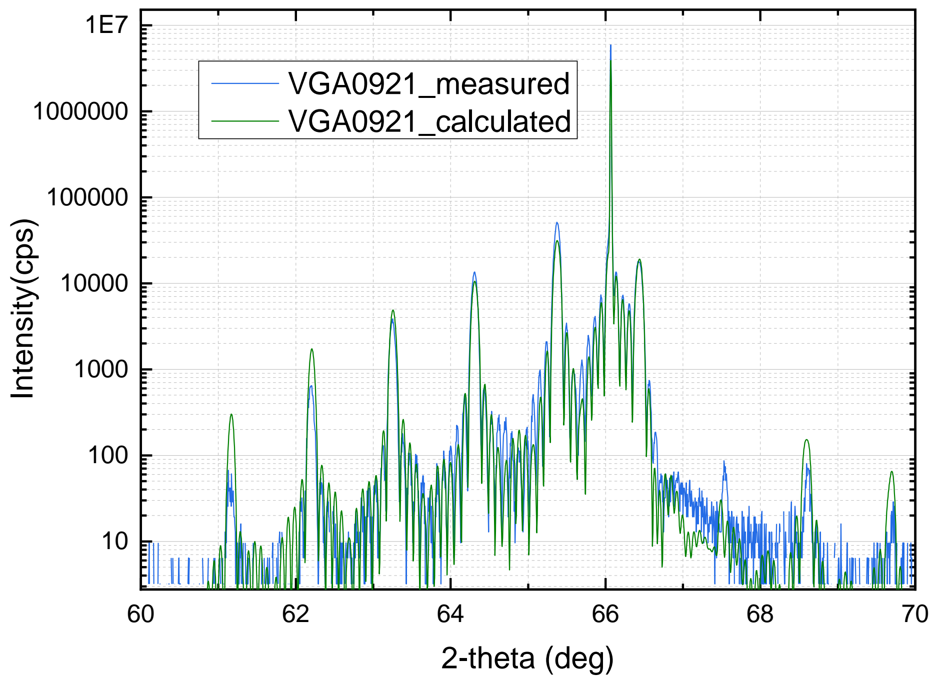

Figure 11. XRD ω-2Θ scan of InGaAs multiple quantum structure (measured sample – blue line; theoretical calculation – green line).

From Fig. 11, it can be observed that the presence of even fringes and narrow diffraction peaks in the resulting 2θ transverse scan indicates that the grown material is of high quality. The results depict accurate well parameter behavior throughout the structure. The experimental rocking curve, compared with the simulated one, further highlighted that the as-grown QW structure exhibited excellent quality structural properties. Overlapping spectra evidence even growth of the structure, while even peaks and dips as well as their width and spaces in between are key factors in modelling accurate quantum well parameters, including width and active material content. The QW thickness and In content established by XRD measurements were presented in Table 1.

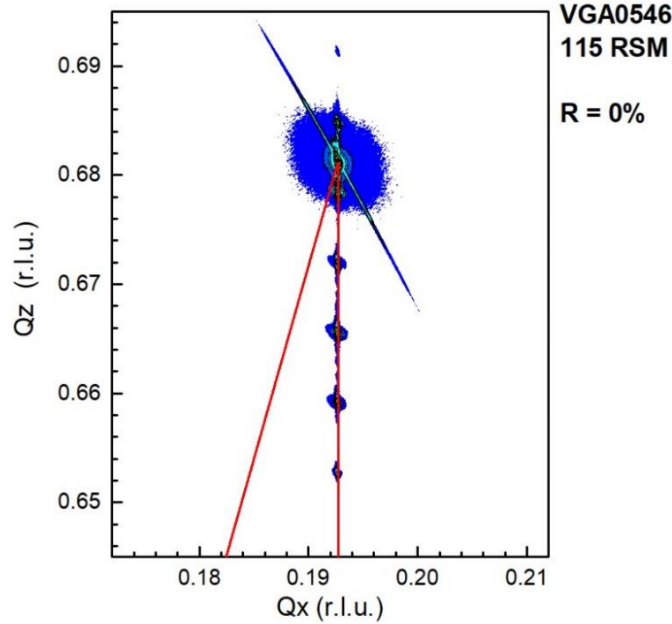

Figure 12. Reciprocal Space Mapping (RSM), depicting a sample with InGaAs (VGA546) quantum wells lattice strain balance. Axes Qx and Qz indicate reciprocal space coordinates. Relaxation value of 0% and the reflections ordered perpendicularly shows that the structure's lattice constant is equivalent to the GaAs substrate lattice constant.

XRD Reciprocal space mapping (RSM) reveals relaxation of the sample. For a particular sample VGA0546, RSM has been measured (Fig. 12). The sample contained 12 quantum wells based on InGaAs as the active material, the parameters of 26% of In content and 4.95 nm width QWs were confirmed by XRD scan. The sample exhibited high PL emission intensity (not shown here) and was chosen for further quality analysis. It can be seen that from the perpendicular zero-reflection behaviour that there is no relaxation. This means that the sample's epitaxial layer and the structure are fully strained – the lateral lattice parameters of the layer are strained to be identical to the substrate's. This ensures the highest quality of the sample structure and is the basis of successful epitaxial growth.

4.3 Photoluminescence measurements

Photoluminescence is arguably the most critical part of optical property analysis. It allows to gain insight into the possible emission of the quantum structure and pinpoint the exact emission wavelength. What is more is that it gives the possibility to oversee any recurring behaviors of the material that become evident through the spectra. This allows to conduct further research towards any novel material or structure mechanisms or study them in a more rigorous manner.

4.3.1 Room temperature PL

The photoluminescence measurements were performed at room temperature using a green (532 nm) DPSS laser with a 0.4 m monochromator. PL signal was detected using a nitrogen-cooled InGaAs point photodetector and the signal was recorded from the lock-in amplifier output. The signal was analyzed in the low photon energy range of 0.9-1.45 eV for all samples. The measurements were essential in determining the accurate emission wavelengths of the structures. This is a basic but a crucial step in assessing the overall quality of the grown structures.

Several samples of both structures have been chosen. Structures containing InGaAs MQWs had varied parameters of 15-26 % of In content and 4-5 nm of QW width. Similarly, samples with GaAsBi QWs had parameters varied between 4-7.5 % of Bi content and 7.9-8.7 nm QW width. While InGaAs MQW samples were grown for emission at around 960–1000 nm, GaAsBi MQW samples were aimed to emit at 1100-1200 nm. The RTPL results are depicted in Figures 13 and 14.

a)

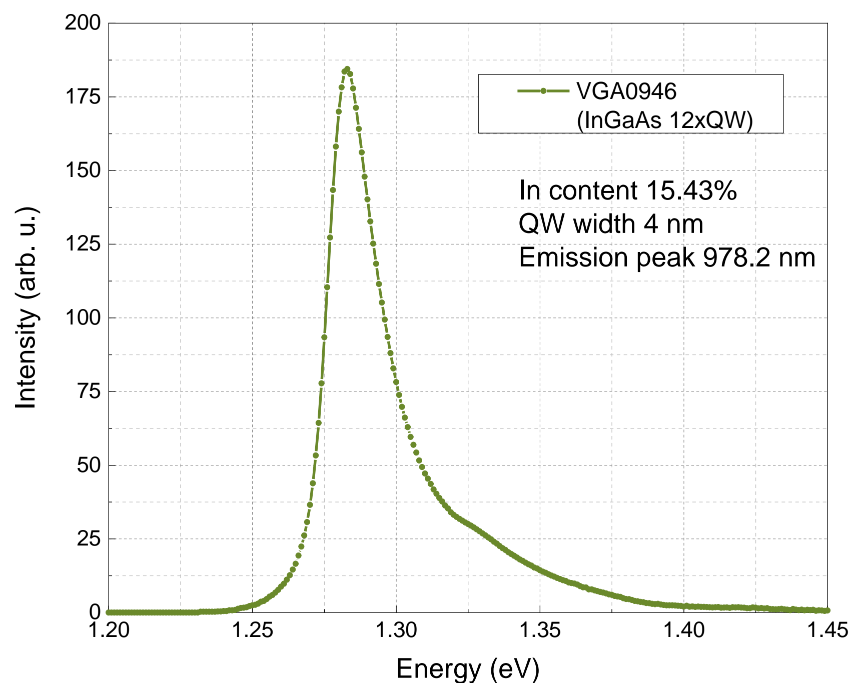

b)

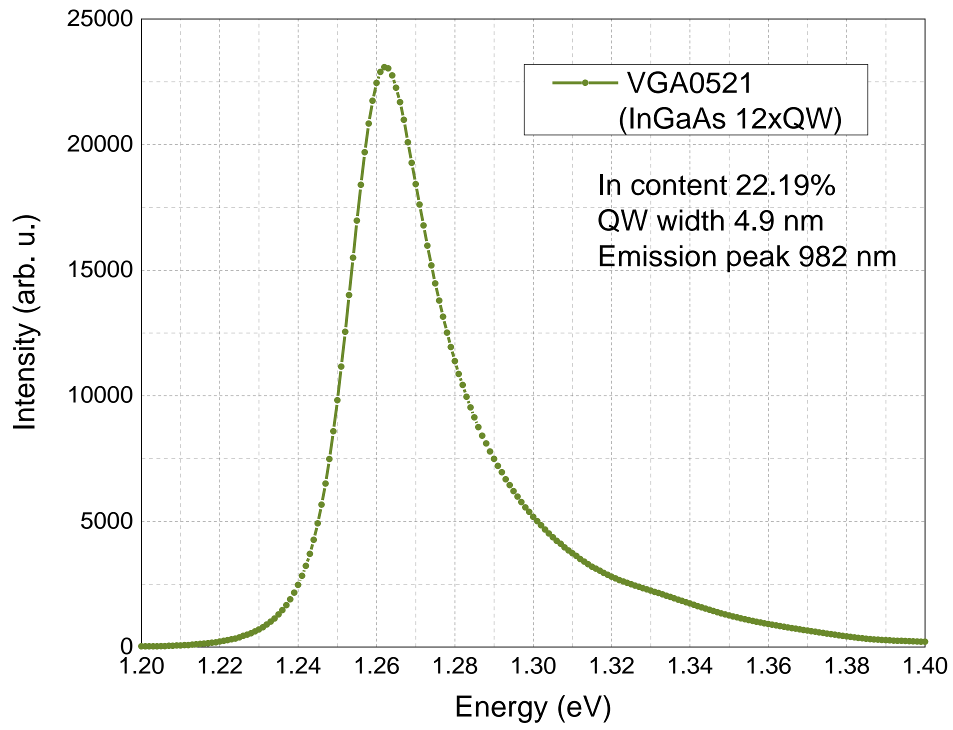

c)

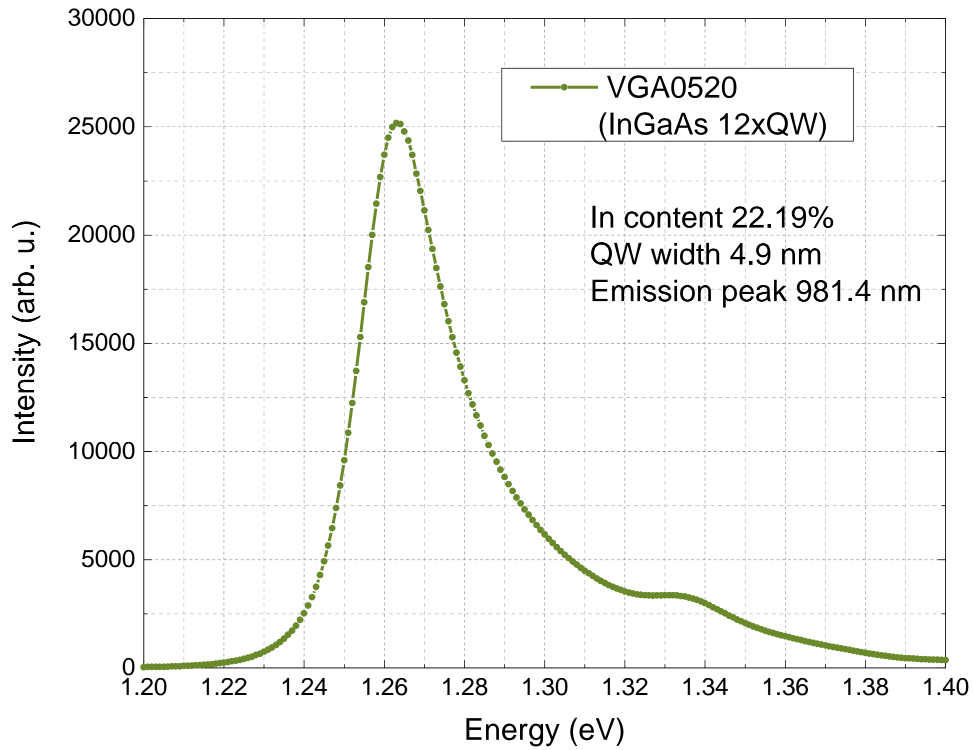

d)

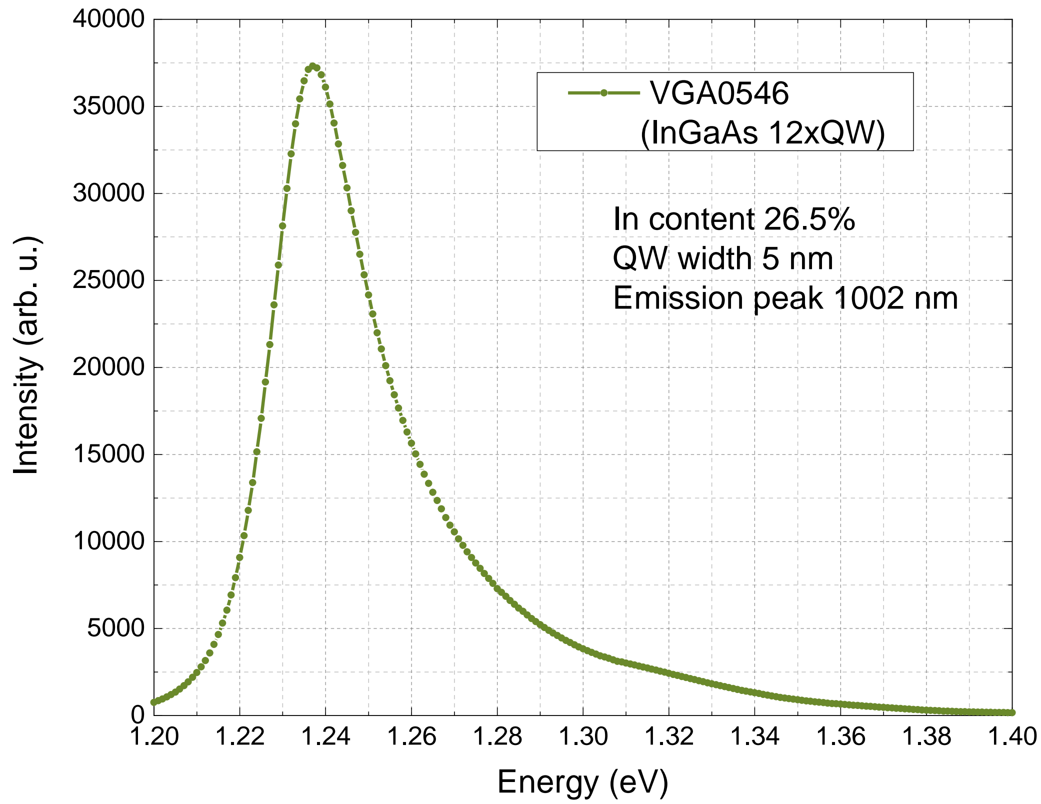

Figure. 13. Samples', containing InGaAs quantum well structures, RT photoluminescence spectra: a) VGA0946; b) VGA0521; c) VGA0520; d) VGA0546. The chosen samples were characterized by different In content and QW width, ranging from 15-26 % and 4-5 nm, respectively. Spectra are characterized according to the peak position, width and the emission intensity. In content and QW width have been deduced from XRD measurement analysis.

a)

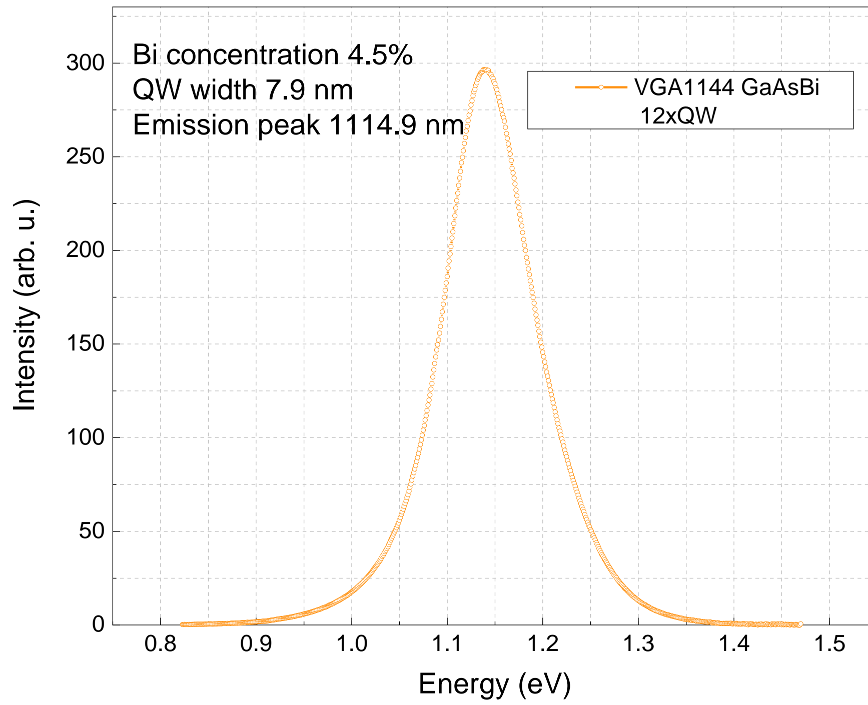

b)

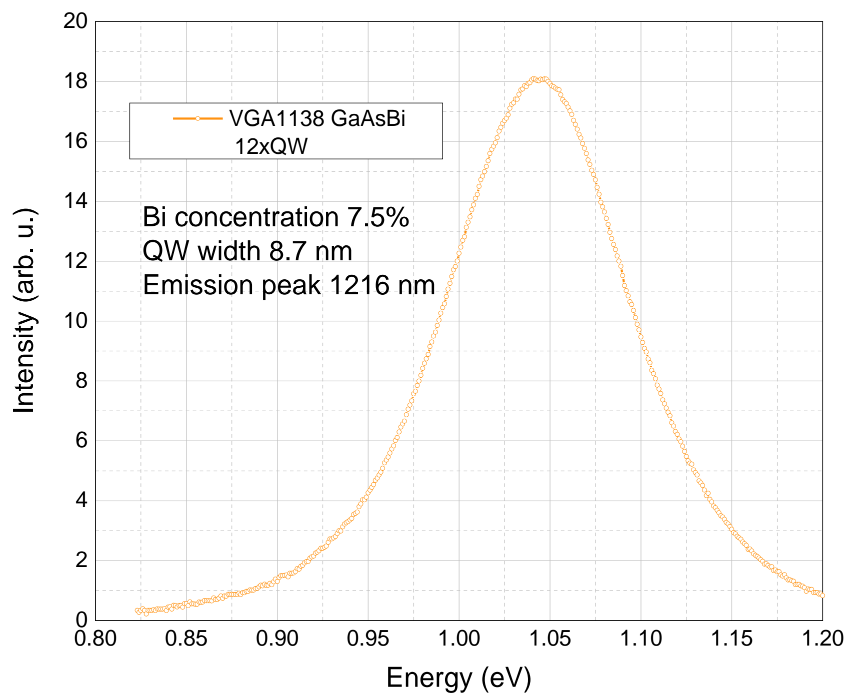

c)

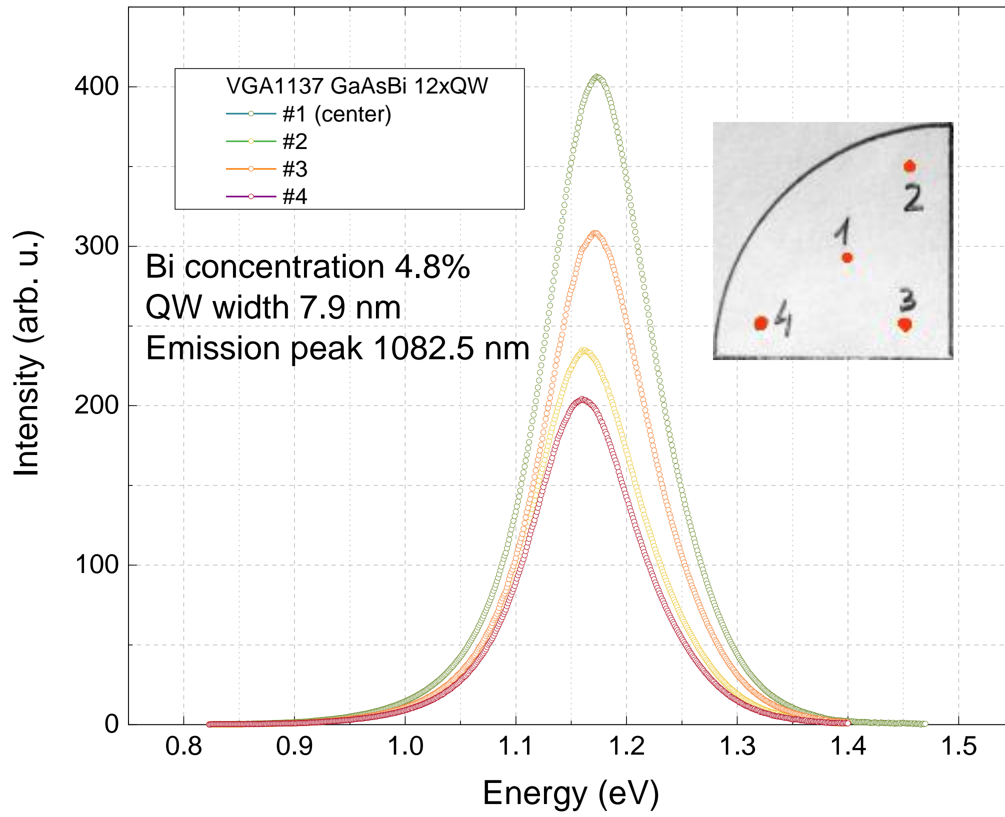

d)

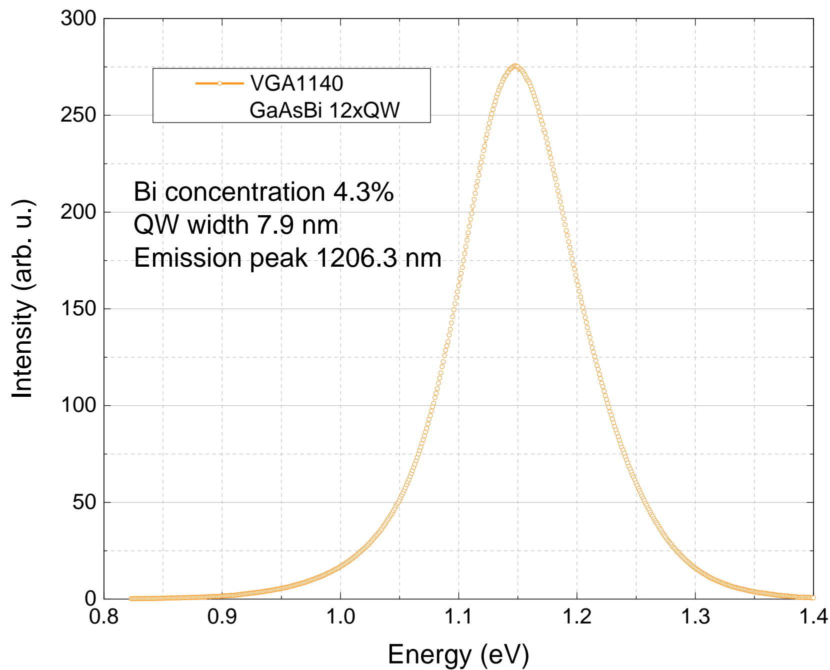

Figure 14. Samples', containing GaAsBi quantum well structures, photoluminescence spectra: a) VGA1144; b) VGA1138; c) VGA1137; d) VGA1140. Spectra are characterized according to the peak position, width and the emission intensity. Bi concentration and QW width have been deduced from XRD scan analysis.

The spectra are observed to shift with the increase of QW width and In content in the structure. Most InGaAs MQW samples have exhibited high intensities of emission, as well as the FWHM of the peaks were as narrow as they were anticipated to be, mostly varying around 16 - 23 meV (depicted in Fig. 13). This deems the samples as high quality structures, as with perfect crystalline and smooth surfaces, emission intensities tend to be higher. It is important to note that two samples, VGA0946 and VGA0520, have exhibited a second peak at around 1.33-1.34 eV. This behaviour is thought to be attributed to the transition from type I to type II for light holes [25]. During the growth of InGaAs containing samples certain trends have been observed that are in favor with literature [26]. With the increase of indium content in quantum wells, as well as increasing their width, the structures' emission shifts towards longer wavelengths. This enables the optimization of the quantum structure growth, in order to target specific wavelengths and grow gain media for VECSELs, emitting at 976, 980, 1060 nm wavelengths.

It is important to know that if a significant amount of point defects form in the sample or the sample contains any other dislocations, nonradiative recombination through defect states may occur. In such case, the relaxed energy transfers to lattice vibrations and heat. This becomes apparent, when photoluminescence spectra peaks drop in intensities. It has also been seen that GaAsBi quantum structure emission peaks are broader than InGaAs structures, most FWHM varying around 100 meV, as GaAsBi growth optimization is significantly more complex (shown in Fig. 14). Characterization of sample VGA1137, containing 12 GaAsBi QWs with 8.7 nm QW width and 4.8% of Bi content, exhibiting emission at 1082 nm, has been done on various spots of the surface. This has led to even further assessment of the qualities of the alloy which will be important for further optimization of the material. Therefore, overall emission range of the samples (at around 1150 nm) as well as high intensities of peak emission do confirm excellent quality samples for applications in the near infrared range.

In general, the results show that the bandgap of GaAsBi QWs with higher Bi incorporation is less sensitive to temperature than the conventional AIII–BV compounds. As such, this behaviour can be described by Varshni parameters that show temperature dependence of structure bandgaps. Most semiconductors tend to exhibit parameter values of around 4 - $6 \cdot 10^{-4}$ eV/deg [27], for example GaAs generally exhibiting $5.4 \cdot 10^{-4}$ eV/deg [28]. Meanwhile GaAsBi QWs have shown values in the order of $3 \cdot 10^{-4}$ eV/deg [28]. The temperature dependencies of these bandgap energies become significantly weak for GaAsBi with Bi incorporation. This suggests that the density of states around the band edge of GaAsBi is modified from that of GaAs due to the localized states possibly originated from Bi clusters. This puts the emphasis on growth conditions of GaAsBi even more as the control of the growth temperatures includes many challenges. Yet the material becomes even more attractive in fiber communication systems.

It was demonstrated that PL results of samples that had higher Bi content have yielded lower emission intensities. Bi incorporation has been deduced from XRD modelling measurements. For example, a clear observation can be done with VGA1138 that has a higher Bi content of 7.5% and exhibits lowest intensities with a broad emission peak. Meanwhile VGA1144 and VGA1153 with Bi concentration of 4.5% and 4.3%, respectively, have shown higher PL intensities and slightly sharper peaks. Such results of the latter two samples might be related a lower density of Ga or As-related defects in structures with less Bi incorporated.

4.3.2 Temperature-dependent PL

TDPL measurements were conducted in a temperature range of 3–300 K. In order to change temperature, the samples were mounted on the cold finger of a closed-cycle He cryostat coupled with a temperature controller. A diode pumped solid-state laser emitting at a wavelength of 532 nm was used as an excitation source at different excitation powers. PL signal was detected with a thermoelectrically cooled InGaAs photodetector using a conventional lock-in system. Two samples were chosen for this method of characterization. Such study was performed to assess the effect of the technological parameters on optical properties. Complex study was performed to clarify the effect of technological parameters on the optical properties. VGA0521 sample structure contained 12 InGaAs QWs and VGA1137 with 12 GaAsBi QWs. The samples were selected as they exhibited high intensity emissions at room temperature and their emission wavelengths were close to desired lasing wavelengths, 982 nm for InGaAs MQWs and 1082 nm for GaAsBi MQWs. The analysis could also depict any changes related to possible defects. The results are shown in Figures 15 and 16.

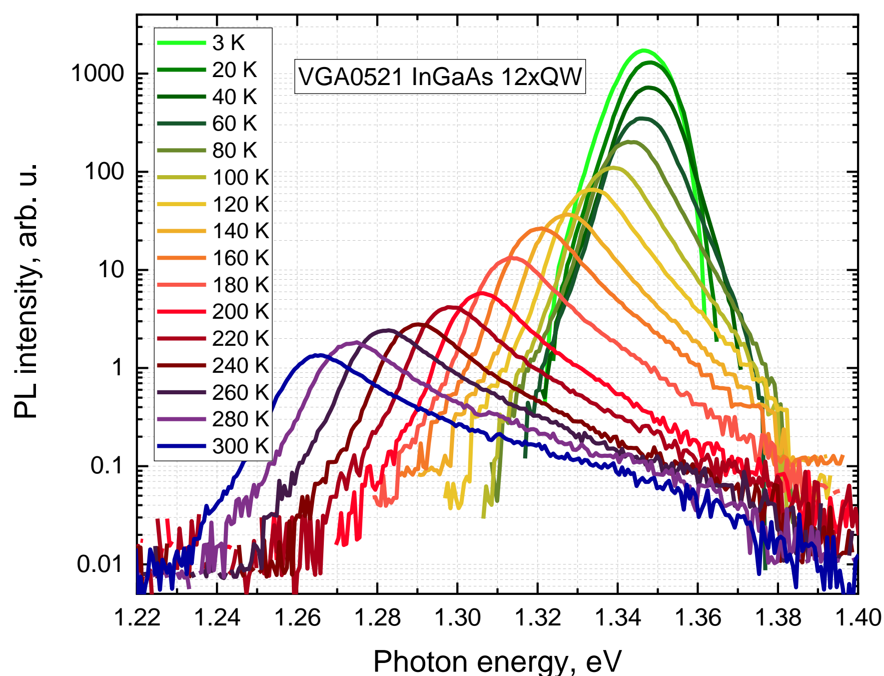

Figure 15. Temperature dependent photoluminescence spectra measured on sample VGA0521 containing 12 InGaAs QWs with parameters of 5 nm QW width and 23.2% of In content.

An obvious shift of photon energies is evident from TDPL measurements of sample VGA0521 (Fig. 15). The sample's structure consisted of 12 InGaAs/GaAs quantum wells, their width set at 5 nm and indium content at 23.2%. A decrease in intensity and a total energy shift of 0.09 eV is observed, across the temperature range from 3 K to 300 K. This concludes the emission wavelength of the structure at 981.6 nm at 300K and at 921.8 nm 3K. This red shift is due to the decreasing of the band gap, i.e., weaker energy bandgap interaction, with increase in temperature due to lattice expansion. Another instance that has been observed of the PL spectra is the distinct change from Gaussian-like to asymmetric line shape, which was induced by the increase in temperature [25]. This might suggest that there is an increased contribution from free carrier recombination with the increase in temperature [29].

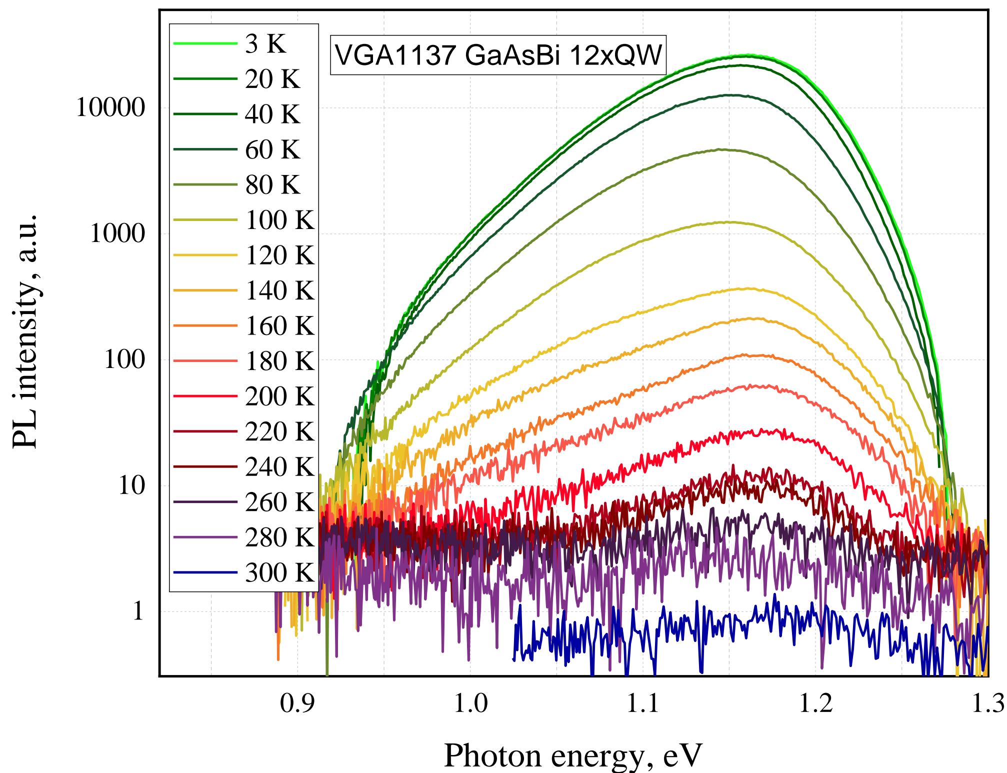

Figure 16. Temperature dependent photoluminescence spectra measured on sample VGA1137 containing 12 GaAsBi QWs with 8.7 nm QW width and 4.8 % of Bi incorporation.

Another PL peak intensity position variation with temperature is shown in Figure 16. Analysing VGA1137 with a structure of a total 12 GaAsBi/GaAs quantum wells of 8.7 nm width with 4.8% Bi incorporation yielded different results. The TDPL depicted a faint shift in photon energies, characterized in an S-shaped dependence, often observed for GaAsBi QW structures and other systems where carrier localization is present [30]–[32]. The initial red shift is caused by a redistribution of excitons over deep localized states, while the blue shift is due to the escape of excitons to delocalized states. The further red shift of the peak PL energy follows the reduction of energy gap with temperature. However, with the increase of temperature, not only did the emission intensities diminish but an increase in noise is evident as well.

4.4 VECSEL structures

With the success of technological optimization of InGaAs and GaAsBi MQWs using MBE, it enabled to continue with the design and growth of the full VECSEL structure. For that, it was important to grow high reflectance (>99.8%) DBR mirrors. Their optimization, growth process and results, not discussed here, were a part of the previous coursework. Implemented DBR structures were shown to be most optimal at 30 pairs of AlAs/GaAs, with high reflectance of the photonic stopband at wavelengths, designed for MQW structures' emission. Therefore, quantum structures have been grown on top the DBR mirrors with AlAs windows to prevent recombination and oxide formation and GaAs capping layers on top to further improve VECSEL qualities.

The structures containing all the required layers of the full VECSEL design, with InGaAs MQW and GaAsBi QW active gain media, are depicted in Figure 17. The growth rate of the InGaAs for the quantum well structure was calculated using RHEED to be at 0.2992 nm/s, meanwhile GaAsBi growth rate was at 0.216 nm/s.

Figure 17. Structural schemes of full VECSEL mirror design containing a) InGaAs MQWs and b) GaAsBi MQWs. Both VECSELs are designed and grown on top of previously grown DBRs with GaAs as the last layer acting together as a buffer. The structures contain 12 QWs with InGaAs and GaAsBi as active material accordingly.

The results of InGaAs and GaAsBi based VECSEL gain regions are discussed as follows. Two structures of different parameters have been chosen. VGA1133 is based on 12 InGaAs QWs with an In content of 22.5 % and QW width of 4.8 nm. Meanwhile VGA1155 contains 12 GaAsBi QWs with 6.3 % of Bi incorporation and their QW width set at 8 nm. Their PL measurements are illustrated below, accordingly with the insets of surface morphology AFM pictures. Due to the peculiarities of both active materials, InGaAs and GaAsBi, different photoluminescence results are observed, in addition with their corresponding AFM measurements. The samples' main emission peaks are at 996 nm and 1097 nm for VGA1133 and VGA1155, respectively.

a)

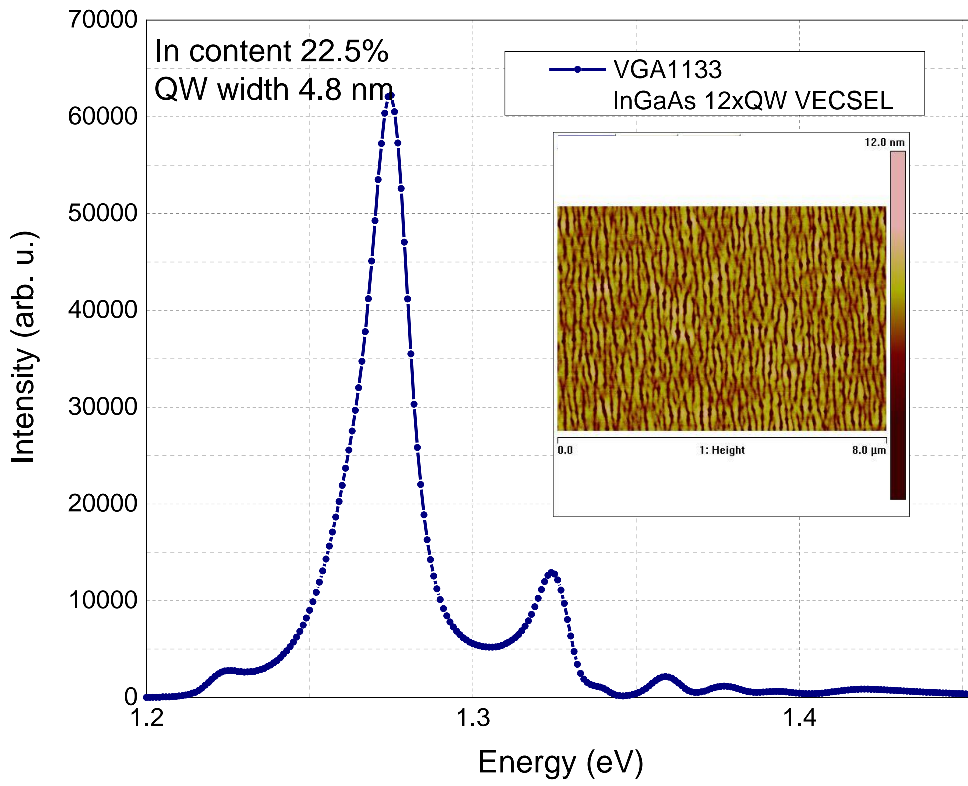

b)

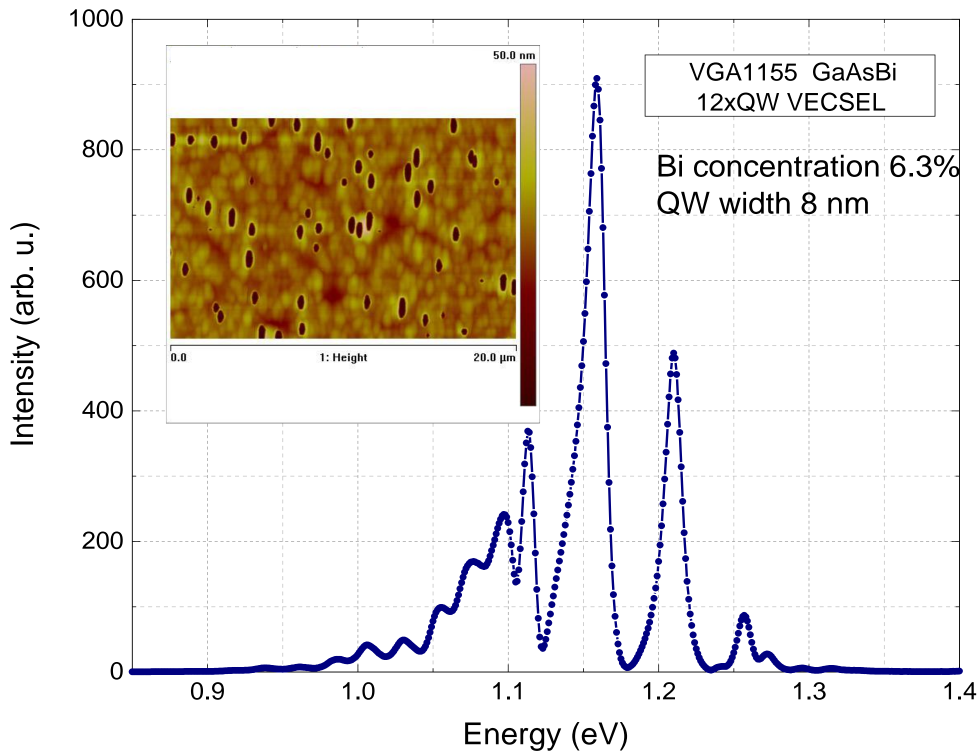

Figure 18. RTPL measurements of VECSEL gain mirror structure, which were grown on DBR, containing a) InGaAs and b) GaAsBi multiple quantum wells as the active material. Insets demonstrate surface morphology of the samples, acquired via atomic force microscopy. The colored scale represents peak-to-peak scale values for height.

Regarding the investigation of the VGA1133 sample structure with InGaAs MQWs, even though the intensities of the emission are favorable, the overall structure still needs further optimization, as the active media emission does not fall within the middle of the DBR bandwidth, targeting the goal emission wavelength (Fig. 18 a). This can be evidenced by the broadened peak of emission from photoluminescence as well as smaller peaks forming towards the sides. This implies that the enhancement of the emission of the quantum structure was not only together with the mirror, but overwhelmingly tracked along the edges of the mirror as well. Meanwhile the AFM measurements of the sample VGA1133 yield particularly good surface results, indicated by small RMS values from the scale and clearly ordered InGaAs domains across all the sample surface.

The intensity of the emission of the VGA1155 sample with GaAsBi MQWs is weaker tenfold compared to the InGaAs structure (Fig. 18 b). The various scattered narrow peaks indicate that due to the positioning of the quantum structure emission wavelength, the DBR bandwidth is not exactly along the center. This means that the mirror reflects and intensifies the edges of the quantum well structure. The morphology of the surface shows typical results for structures with GaAsBi compounds. Evident are GaAs caping layer pits, of around 40-50 nm depth and around 500 nm width, formed across all over the sample surface, which do not necessarily diminish the overall optical qualities of the structure.

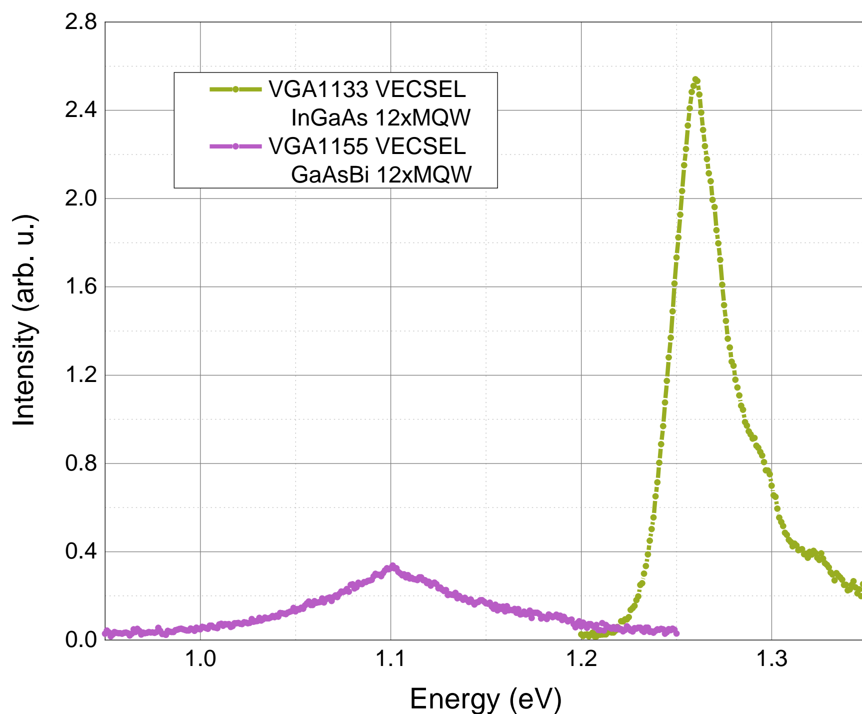

Figure 19. Photoluminescence measurements at room temperature of both VECSEL structures, VGA1133 and VGA1155, containing InGaAs MQWs and GaAsBi MQWs, respectively. The excitation using 190 mW 532 nm laser has been performed on the structure from the edge, i.e., exciting only the quantum wells.

Additional investigation has been done using photoluminescence method but instead of exciting the structure from the top of it, the laser excitation is directed from the edge of the structure, precisely at the quantum structure. This yields most accurate position of the emission of the structure which is essential for positioning the DBR with the emission of the quantum wells.

The results are depicted in Figure 19. It is worth noting that in this case, the intensities of the emission are not important. The intensities are low due to tiny excitation area, thereby the most important aspect of said experiment is the correct and accurate positioning of the bandwidth. Using this method of photoluminescence excitation, emission wavelengths of the according structures are therefore 1.26 eV for InGaAs MQW VECSEL and 1.01 eV for GaAsBi MQW VECSEL. Comparing these acquired results with previously done PL measurements, where the excitation has been performed on top of the structure, some discrepancies can be already observed. For InGaAs MQW structure the difference appears to be nominal of only 14 meV and 149 meV for GaAsBi MQW based VECSEL. This essentially yields more information for comparisons with DBR bandwidth and future growth of such structures as it allows better alignment of the target wavelength windows.

Further improvements are to be expected regarding technological qualities of the structures as well as thorough chip testing is needed to confirm and assess lasing properties.

5. Conclusions

The purpose of this work was by determining the appropriate growth conditions for quantum structures and optimizing their growth procedure to produce high quality MQW structures based on InGaAs and GaAsBi that would be based in NIR laser devices. This led to an in-depth investigation of the properties based on growth conditions of the structures.

Main work conclusions can be structuralized into two parts: (1) technological optimization of quantum structures containing InGaAs and GaAsBi MQWs and their characterization and (2) VECSEL design and importance of implemented structures:

- ❖ Full optimization of technological MBE parameters led to successful growth of InGaAs and GaAsBi based MQW structures on GaAs platform, tailoring their emission wavelengths for 760-1060 nm and 1000-1200 nm, respectively.
- ♦ GaAsBi/GaAs MQW as an active area:

  1. The technological parameter optimization led to successful growth of 12xMQW structures, containing GaAsBi/GaAs as the active material. The optimization emphasized the importance of low substrate temperatures, not higher than 425°C, and the need of stable Ga and As flux ratio for high crystalline and homogenous (distribution of Bi%) growth. The MQW structures exhibited highest PL emissions at around 5% of Bi content, emitting at 1100-1150 nm grown using As/Ga flux ratio of 0.9-0.98.
  2. AFM results have shown GaAsBi surface imperfections: problems with metallic surface droplets and pits were encountered, which allude to the limits of the amount of Bi that could be incorporated into the QW.

  Note: While the ability to tune the emission energy of GaAsBi with little amounts of Bi incorporation has been proven, it still poses a problem in controlling good surface quality with high emission intensities. TDPL and AFM measurements have emphasized the need to further improve growth qualities as well as to suppress Auger recombination and inter-valence band absorption at higher Bi concentrations, when the splitting energy exceeds the bandgap (above ~10% Bi content).

- InGaAs/GaAs MQW as an active area:

  1. The technological parameter optimization also led to successful growth of 12xMQW structures, containing InGaAs/GaAs as the active material. Highest emissions with smooth surfaces were analyzed for structures emitting at 960-980 nm wavelength and with higher In content of around 22-26 %. These fully strained structures also favored thinner QWs of around 4 nm thickness.
  2. Majority of the InGaAs MQW samples have exhibited high intensities of PL emission, as well as narrow FWHM around 16-23 meV. This deems the samples as high-quality structures, exhibiting perfect crystallinity and smooth interfaces, emission intensities significantly higher (more than few thousandfold) when compared to lower quality structure emissions.
  3. The emission wavelength of InGaAs tends to red shift with both the increase of In content and QW width. Results have shown that it is possible to achieve intense emission at 970 nm with 14% of In content and 4 nm QWs, meanwhile longer wavelengths of 1000 nm require around 24-26% of In incorporation with QW width not less than 5 nm.

- An important part of the VECSEL design lies in the DBR design, able to enhance the emission and make high output lasing possible. However, the most integral part of the laser is the quantum structures as it places a foundation on the desired properties of the laser. Summarizing the growth and investigation of VECSEL structures, the following can be concluded:

  Optimal DBR structures contain 30 pairs of GaAs/AlAs layers and exhibit high reflectance >99.8% with a plateau of the photonic stopband in order of 100 nm centered at wavelengths designed for InGaAs and GaAsBi MQWs.

  1. Fully designed and grown VECSEL structures exhibited high emissions at 1000 nm for the VECSEL based on 12xInGaAs/GaAs QWs and at 1100 nm - for the 12xGaAsBi/GaAs QW based VECSEL. MQW structures were grown using fully optimized growth conditions previously concluded.
  2. Excitation from the edge of the structure proved to be beneficial in order to determine the correct positioning of the emission.

These results are extremely important when considering InGaAs and GaAsBi based quantum structures to be implemented in NIR laser diodes and VECSELs. As such, obtaining high quality epitaxially grown multiple quantum well structures that would simultaneously exhibit smooth surfaces and high luminescence intensities at desired wavelengths is critical for novel, high performance VECSELs and can be thoroughly realized with proper selection and control of growth conditions. Following crucial steps include thorough chip testing and assessing laser properties. These results open good prospects for further work at developing structures for applications of VECSEL devices.

Bibliography

[1] M. Kuznetsov, VECSEL semiconductor lasers: A path to high-power, quality beam and UV to IR wavelength by design, *Semiconductor Disk Lasers: Physics and Technology, Wiley-VCH (2010)*

[2] K. Nechay, High-Power VECSELs Operating at the 700-800 nm Wavelength Range, *Doctoral Dissertation, Tampere University (2019).*

[3] M. Guina, A. Rantamäki, and A. Härkönen, "Optically pumped VECSELs: Review of technology and progress," *J. Phys. D. Appl. Phys.*, vol. 50, no. 38, 2017.

[4] A. C. Tropper, H. D. Foreman, A. Garnache, K. G. Wilcox, and S. H. Hoogland, "Vertical-external-cavity semiconductor lasers," *J. Phys. D. Appl. Phys.*, vol. 37, no. 9, pp. 75–85, 2004.

[5] E. O. Odoh and A. S. Njapba, "A Review of Semiconductor Quantum Well Devices," *Adv. Phys. Theor. Appl.*, vol. 46, pp. 26–32, 2015.

[6] Hartmut Haug; Stephan W. Koch, Quantum Theory of the Optical and Electronic Properties of Semiconductors, *World Scientific (2007).*

[7] Dieter Bimberg, "Quantum dots for lasers, amplifiers and computing," *J. Phys. D: Appl. Phys.* 38 2055 (2005).

[8] A. Ghadimi and M. Ahmadzadeh, "Effect of Variation of Specifications of Quantum Well and Contact Length on Performance of Inp-Based Vertical Cavity Surface Emitting Laser (VCSEL)," vol. 5, no. 1, 2020.

[9] M. Guina, T. Leinonen, A. Härkönen, and M. Pessa, "High-power disk lasers based on dilute nitride heterostructures," *New J. Phys.*, vol. 11, Dec. 2009.

[10] K. Oe and H. Okamoto, "New Semiconductor Alloy $GaAs_{1-x}Bi_x$ Grown by Metal Organic Vapor Phase Epitaxy," *Japanese Journal of Applied Physics* vol. 37, no. 11, Nov. 1998.

[11] E. C. Young, S. Tixier, and T. Tiedje, "Bismuth surfactant growth of the dilute nitride GaN_xAs_{1-x}," *J. Cryst. Growth*, vol. 279, no. 3–4, pp. 316–320, Jun. 2005.

[12] B. Vahid Bahrami Yekta, "Optimization of growth conditions of GaAs1-xBix alloys for laser applications," *Doctoral Dissertation, University of Victoria*, 2016.

[13] P. J. A. Thijs, L. F. Tiemeijer, P. I. Kuindersma, J. J. M. Binsma, and T. Van Dongen, "High-Performance 1.5 μM Wavelength Ingaas-Ingaasp Strained Quantum Well Lasers and Amplifiers," *IEEE J. Quantum Electron.*, vol. 27, no. 6, pp. 1426–1439, 1991.

[14] A. R. Adams, "Strained-layer quantum-well lasers," *IEEE J. Sel. Top. Quantum Electron.*, vol. 17, no. 5, pp. 1364–1373, 2011.

[15] L. Morresi, "Basics of molecular beam epitaxy (MBE)," *Silicon Based Thin Film Sol. Cells*, no. January 2013, pp. 81–107, 2013.

[16] A. A. Allerman, T. D. Raymond, and W. J. Alford, "High power and good beam quality at 980 nm from a vertical external-cavity surface-emitting laser," *JOSA B, Vol. 19, Issue 4, pp. 663-666*, vol. 19, no. 4, pp. 663–666, Apr. 2002.

[17] S. J. Sweeney and S. R. Jin, "Bismide-nitride alloys: Promising for efficient light emitting devices in the near- and mid-infrared," *J. Appl. Phys.*, vol. 113, no. 4, p. 043110, Jan. 2013.

[18] John C. Woolley, Mathew B. Thomas, and Alan G. Thompson. Optical energy gap variation in Ga_xIn_{1-x} As alloys. *Canadian Journal of Physics*. 46(2): 157-159, 1968.

[19] B. R. Nag, Physics of Quantum Well Devices, Solid-State Science and Technology Library, edited by L. R. Carley, G. Declerck, and F. M. Klaassen (*Kluwer Academic Publishers, Dordrecht, 2000*), Vol. 7, p. 41, 53.

[20] Wolfgang Braun, Applied RHEED, *Springer Berlin Heidelberg*, 1999.

[21] R. Butkute, V. Pačebutas, A. Krotkus, N. Knaub, and K. Volz, "Migration-enhanced epitaxy of thin GaAsBi layers," *Lith. J. Phys.*, vol. 54, no. 2, pp. 125–129, Jun. 2014.

[22] K. Alberi, O. D. Dubon, W. Walukiewicz, K. M. Yu, K. Bertulis, and A. Krotkus, "Valence band anticrossing in $GaBi_xAs_{1-x}$," *Appl. Phys. Lett.*, vol. 91, no. 5, p. 051909, Jul. 2007.

[23] N. A. Riordan *et al.*, "Temperature and pump power dependent photoluminescence characterization of MBE grown GaAsBi on GaAs," *J. Mater. Sci. Mater. Electron. 2012 2310*, vol. 23, no. 10, pp. 1799–1804, Mar. 2012.

[24] X. Lu, D. A. Beaton, R. B. Lewis, T. Tiedje, and M. B. Whitwick, "Effect of molecular beam epitaxy growth conditions on the Bi content of $GaAs_{1-x}Bi_x$," *Appl. Phys. Lett.*, vol. 92, no. 19, p. 192110, May 2008.

[25] A. C. Tropper and S. Hoogland, "Extended cavity surface-emitting semiconductor lasers," *Prog. Quantum Electron.*, vol. 30, no. 1, pp. 1–43, 2006.

[26] T. Lin *et al.*, "Material research on the InGaAs-emitting-layer VECSEL grown on GaAs substrate," *Mater. Sci. Semicond. Process.*, vol. 42, pp. 283–287, 2016.

[27] R. Pässler, "Semi-empirical descriptions of temperature dependences of band gaps in semiconductors," *Phys. status solidi*, vol. 236, no. 3, pp. 710–728, Apr. 2003.

[28] E. Dudutienė *et al.*, "Photoluminescence properties of GaAsBi single quantum wells with 10% of Bi," *Lith. J. Phys.*, vol. 61, no. 2, pp. 142–150, Jun. 2021.

[29] L. Xu, D. Patel, C. S. Menoni, J. Y. Yeh, L. J. Mawst, and N. Tansu, "Optical determination of the electron effective mass of strain compensated $In_{0.4}Ga_{0.6}As_{0.995}N_{0.005}$/GaAs single quantum well," *Appl. Phys. Lett.*, vol. 89, no. 17, 2006.

[30] R. Kudrawiec, M. Latkowska, M. Baranowski, J. Misiewicz, L. H. Li, and J. C. Harmand, "Photoreflectance, photoluminescence, and microphotoluminescence study of optical transitions between delocalized and localized states in $GaN_{0.02}As_{0.98}$, $Ga_{0.95}In_{0.05}N_{0.02}As_{0.98}$, and $GaN_{0.02}As_{0.90}Sb_{0.08}$ layers," *Phys. Rev. B - Condens. Matter Mater. Phys.*, vol. 88, no. 12, p. 125201, Sep. 2013.

[31] A. Kaschner, T. Lüttgert, H. Born, A. Hoffmann, A. Y. Egorov, and H. Riechert, "Recombination mechanisms in GaInNAs/GaAs multiple quantum wells," *Appl. Phys. Lett.*, vol. 78, no. 10, p. 1391, Feb. 2001.

[32] S. Baranovskii, R. Eichmann, and P. Thomas, "Temperature-dependent exciton luminescence in quantum wells by computer simulation," *Phys. Rev. B*, vol. 58, no. 19, p. 13081, Nov. 1998.

Summary

Optimization of Quantum Structure Technology for Near Infrared Laser Sources

Silvija Keraitytė

Various lasers, including solid-state, semiconductor, gas lasers are used in many fields such as optical fibre communication, material processing, biology, spectroscopy. Different applications usually require unique laser parameters: beam quality, wavelength tunability, compact size, high optical output power etc. Vertical-external-cavity surface-emitting laser (VECSEL) also called optically pumped semiconductor laser (OPSL) or semiconductor disk laser (SDL) belong to a new generation laser family that combines many of the desirable properties and were first developed to overcome key problems typical to conventional semiconductor lasers. A crucial part of a VECSEL is the distributed Bragg reflector (DBR), defined as the external mirror. However, the most important structure is the gain region based on quantum wells. This part of the laser determines the main properties of the laser. The parameters and quality of the active gain region can be tuned with specific QW growth conditions and correct materials. For NIR laser sources, main active materials were chosen to be InGaAs and GaAsBi MQWs grown on GaAs substrate.

In this work the growth of structured DBR was performed using solid-source MBE system (Veeco GENxplor R&D and SVT-A) equipped with standard cells for metallic aluminium, indium, gallium, and unique arsenic design source generating pure arsenic dimers flux. The aim of this work was to determine the appropriate growth conditions for quantum structures, and successfully grow quantum wells based on InGaAs and GaAsBi materials, tailoring the wavelength to 760 – 1030 nm and 1000 - 1200 nm, respectively. The process has led to a thorough investigation of effect of growth conditions on GaAsBi and InGaAs optical properties, including full characterization using PL, AFM, XRD methods. The work has been concluded by designing a full VECSEL gain chip based on InGaAs and GaAsBi MQWs and assessing their optical properties.

This paves a way for future designs of structures and implementation possibilities for VECSELs and NIR devices. Any further device testing and electrical characterization will base further work.

Santrauka

Kvantinių struktūrų, skirtų artimosios infraraudonosios srities lazeriniams šaltiniams, technologijos optimizavimas

Silvija Keraitytė

Šiandien įvairūs lazeriai, tokie kaip, kietakūniai, puslaidininkiniai, dujiniai, yra sėkmingai naudojami daugelyje sričių, telekomunikacijos, medžiagų apdorojime, biologijoje, spektroskopijoje ir t.t. Skirtingiems taikymams keliami skirtingi reikalavimai lazerių parametrams: spinduliuojamo bangos ilgio perderinamumas, skleidžiamo pluošto kokybė ir forma, optinė galia, prietaiso dydis ir kt. Optiškai kaupinami VECSEL priklauso naujos kartos lazerių šeimai, kuri ir apjungia daugumą išvardintų patrauklių savybių. Tačiau daugumai tokių taikymų rinkoje parduodami šaltiniai pasižymi standartiniais parametrais, nėra labai efektyvūs, nes patiria nuostolius dėl nespindulinės Auger rekombinacijos ir dėl elektronų šuolių tarp skirtingų valentinės juostos šakų, be to jie yra labai jautrūs temperatūros pokyčiams. Taigi naujų stabilesnių medžiagų, veikiančių kambario temperatūroje NIR spektrinėje srityje, inžinerija ir tyrimas vis dar yra labai aktualūs.

Darbo tikslas yra optimizuoti A3-B5 kvantinių darinių technologiją pritaikant ją artimosios infraraudonosios srities šaltinių aktyviojoje terpėje. Šiam tikslui bus auginami ir tiriami InGaAs ir GaAsBi kvantiniai dariniai. Numatoma kvantinių darinių emisijos bangos ilgių sritis - nuo 760 nm iki 1200 nm. Visos struktūros buvo užaugintos naudojantis molekulinių pluoštų epitaksija (MBE). Atliktas sudėtinis išaugintų kvantinių struktūrų tyrimas, siekiant išryškinti svarbiausius technologinius parametrus, turinčius įtakos struktūrų optinėms savybėms. Rezultatai parodė, atlikus auginimo proceso optimizavimą, galima pasiekti aukštos kokybės kvantinių struktūrų darinius. Darbe taip pat buvo užauginta pilnos VECSEL struktūros, remiantis InGaAs bei GaAsBi kvantinėmis duobėmis ir dizainu, atitinkančiu aukštos kokybės lazerio veikimą. Struktūros buvo išanalizuotos ir įvardintos jų optinės savybės bei trūkumai.

Optiniai užaugintų struktūrų tyrimai leido įvardinti problemines technologijos sritis ir atskleisti puslaidininkinių darinių auginimo sąlygų ir optinių savybių sąsajas. Šie rezultatai yra ypač svarbūs tolesniems darbams, o ištirtos medžiagos leis toliau tobulinti struktūras, kurios reikalingos aukštos galios VECSEL ir NIR prietaisams.